

QATAR UNIVERSITY

COLLEGE OF ARTS AND SCIENCES

PROSPECTS OF BIOCRUDE PRODUCTION POTENTIAL FROM LOCAL DIATOM

BY

SARA MOHAMMED AL-NAIMI

A Thesis Submitted to

the College of Arts and Sciences

in Partial Fulfillment of the Requirements for the Degree of

Masters of Science in Master of Science in Environmental Sciences

June 2020

© 2020. Sara. All Rights Reserved.

## COMMITTEE PAGE

The members of the Committee approve the Thesis of  
Sara defended on [Defense Date].

---

Dr. Abdurhman Al Muftah  
Thesis/Dissertation Supervisor

---

Dr. Probir Das  
Committee Member

---

Dr.Mohammed Alghouti  
Committee Member

---

Dr. Imen Saadaoui  
Committee Member

---

Add Member

Note: the empty committee member names should be removed.

Approved:

---

Ibrahim AlKaabi, Dean, College of Arts and Sciences

## ABSTRACT

AL-NAIMI, SARA, MO., Masters : June : 2020,

Master of Science in Environmental Sciences

Title: PROSPECTS of BIOCRUDE PRODUCTION POTENTIAL FROM LOCAL DIATOM

Supervisor of Thesis: Dr. Abdurhman, Mo, Al Muftah.

A marine diatom *Nitzchia reversa* was grown in 5 sq. m open raceway pond (10 cm culture depth, 500 L culture volume) in the Qatari desert environment. After 7 days of growth, the final biomass density reached 0.52 g/L, and average biomass productivity was 6.7 g/m<sup>2</sup>/d. Next, *Nitzchia reversa* was harvested using a 25 m<sup>2</sup> crossflow filtration membrane module. Crossflow harvested biomass slurry was centrifuged at 5000 RPM for 10 minutes to obtain a wet biomass paste containing 25 - 30% solid content. Centrifuged biomass was freeze-dried, and lipid, protein, carbohydrate, and ash were quantified as 12.3, 15.3, 44.3, and 27.8% respectively. Hydrothermal liquefaction (HTL) was conducted to convert *Nitzchia reversa* biomass to biocrude oil using 10-mL Swagelok union type reactors. Biocrude, biochar, aqueous and gas phase were quantified on an ash-free dry weight basis. Hydrothermal liquefaction was conducted at temperatures ranging from (300, 325, 350, 375, and 400 °C) at 30-minute reaction holding time, maximum biocrude yield of 57.26% was obtained at 375 °C. Carbon content within the biocrude decreased with increasing HTL reaction temperature, whereas, oxygen content increased with increasing HTL reaction temperature. The maximum higher heating value for biocrude oil was 35.1 MJ/kg at 300 °C. Hydrocarbons in biocrude were identified as alkanes, alkenes,

aromatics, and heterofunctional groups by GC-MS. However, high biocrude yields could be obtained from *Nitzchia reversa* with increasing HTL reaction temperatures with maximum energy recovery (ER) of 53.01% at 375 °C.

## DEDICATION

*This study is dedicated to my daughter Haya*

## ACKNOWLEDGMENTS

It is a genuine pleasure to express my deep sense of thanks and gratitude to my advisor Dr. Abdurhman Al-Muftah for his continuous support, guidance, and encouragement throughout this journey. I would also like to thank my co-supervisor Dr. Mohammed Al-Ghouti for his valuable comments on my thesis. I'm sincerely grateful to Dr. Probir for playing a significant role in paving the way that led me to where I am now. I appreciate his vast experience and willingness to improve my knowledge. I would also like to extend my appreciation to Dr. Hareb Aljabri and the ATP staff; Ms. Ghomza, Mr. Mohammed AbdulQadir, and Mr. Shoyb for their effort in helping me get the most out of this experience. In addition, a thank you to Dr. Iman, Ms. Tasneem, Ms. Thuria, Ms. Rehab, and Ms. Marwa and Mr. Mahrouf, for assisting me through all the necessary analyses. Also, I want to acknowledge The Environmental Study Center and Central Lab Units facility members for their assistance. Finally, I would like to acknowledge with gratitude the support and encouragement of my loving family and friends.

## TABLE OF CONTENTS

DEDICATION .....	v
ACKNOWLEDGMENTS .....	vi
LIST OF TABLES .....	x
LIST OF FIGURES .....	xi
LIST OF EQUATIONS .....	xiii
<b>Chapter 1: INTRODUCTION</b> .....	<b>1</b>
<b>Chapter 2: LITERATURE REVIEWS</b> .....	<b>2</b>
<b>Chapter 3: MATERIALS AND METHODOLOGY</b> .....	<b>16</b>
<b>Materials</b> .....	<b>16</b>
<b>Media preparations</b> .....	<b>16</b>
<b>Solutions and reagents</b> .....	<b>18</b>
<b>Kits</b> .....	<b>18</b>
<b>Methods :</b> .....	<b>19</b>
<b>Collection</b> .....	<b>19</b>
<b>Isolation and purification of the diatom strains performed as it described in (Robert A. Andersen, 2005)</b> .....	<b>19</b>
<b>Screening of diatom strains</b> .....	<b>20</b>
<b>Optimization of salinity levels on diatom growth</b> .....	<b>20</b>
<b>Optimization of nitrogen source on diatom growth</b> .....	<b>21</b>

<b>Optimization of nitrogen concentration on diatom growth</b> .....	21
<b>Pre-cultivation of inoculum in indoor systems</b> .....	22
<b>Mass cultivation of inoculum in open pond system</b> .....	23
<b>Microalgae harvesting performed as described by (P. Das et al., 2019)</b> .....	24
<b>Lipid content and fatty acid methyl esters (FAMES)</b> .....	25
<b>Quantitative analysis of lipids using sulfo-phospho-vanillin as described by (Byreddy et al., 2016)</b> .....	26
<b>Quantitative analysis of protein using Lowry method performed as it was described by (López et al., 2010)</b> .....	26
<b>Quantitative analysis of total carbohydrates by phenol-sulfuric acid colorimetric assay performed as it described by (Dubois et al., 1951)</b> .....	27
<b>Ash Content performed as it was described by (Probir Das et al., 2020)</b> .....	28
<b>Hydrothermal liquefaction experiment</b> .....	29
<b>Biochar content performed as described by (Probir Das et al., 2020)</b> .....	30
<b>Quantitative analysis of biocrude</b> .....	30
<b>Calorific values and CHNS analysis performed as described by (P. Das et al., 2019)</b> .....	30
<b>GC–MS analysis</b> .....	30
<b>Determining energy recovery and energy return on investment as described by (Liu et al., 2018; Yoo et al., 2015)</b> .....	31
<b>Pigment quantification</b> .....	31



<b>Statistical Analysis</b> .....	32
<b>Chapter 4: RESULTS AND DISCUSSION</b> .....	34
<b>Screening of diatom strains</b> .....	34
<b>Optimization of salinity levels on diatom growth</b> .....	35
<b>Optimization of nitrogen source on diatom growth</b> .....	36
<b>Optimization of nitrogen concentration on diatom growth</b> .....	38
<b>Characterization of <i>Nitzchia reversa</i> biomass</b> .....	40
<b>Biochemical composition of <i>Nitzchia reversa</i> biomass</b> .....	42
<b>Lipid content and fatty acid methyl esters (FAMES) of <i>Nitzchia reversa</i> biomass</b> .....	44
<b>Effect of hydrothermal liquefaction operating temperature on the products</b> ..	47
<b>Operating temperature</b> .....	47
<b>Higher heating values of the biocrude</b> .....	51
<b>Distribution of hydrocarbons in the biocrude obtained from hydrothermal     liquefaction</b> .....	56
<b>Energy recovery potential</b> .....	58
<b>Chapter 5: Conclusion</b> .....	61
References.....	62
Appendix: GC/MS chromatogram of (FAMES) .....	78
Appendix: GC/MS chromatogram of hydrocarbons in the biocrude.....	78

Appendix: fucoxanthin wavelength .....	81
--	----

## LIST OF TABLES

Table 1: Cell density, growth rate, biomass, lipid content, and fucoxanthin content of marine diatoms cultivated under different mediums. ....	9
Table 2: An overview of studies investigating biocrude yield produced from microalgal HTL.....	14
Table 3: Composition of F/2 growth medium.....	16
Table 4: F/2 Trace metal solution .....	17
Table 5: Vitamin Solution.....	17
Table 7: Light microscopy image of a <i>Trachyneis aspera</i> , <i>Nitzchia reversa</i> , and <i>Amphora sp.</i> culture 100X magnification.....	34
Table 8: Elemental analysis, ash, and HHV of the <i>Nitzchia reversa</i> biomass.....	41
Table 9: Fatty acid composition and profile of <i>Nitzchia reversa</i> .....	46

## LIST OF FIGURES

Figure 1: An overall reaction mechanism for HTL of microalgae .....	11
Figure 2: Raceway pond .....	24
Figure 3: Tangential flow filtration (TFF) unit.....	25
Figure 4: 10 mL high-pressure Swagelok fitting type reactors.....	29
Figure 5: Methodology scheme diagram of this study.....	33
Figure 6: The growth of <i>Nitzschia reversa</i> (top) and <i>Amphora sp.</i> (bottom) under different salinity concentrations (error bar presents standard error where n =2).....	36
Figure 7: The growth of <i>Nitzschia reversa</i> (top) and <i>Amphora sp.</i> (bottom) under different nitrogen sources (error bar presents standard error where n =2) .....	38
Figure 8: The growth of <i>Nitzschia reversa</i> (top) and <i>Amphora sp.</i> (bottom) under different sodium nitrate concentrations (error bar presents standard error where n =2) .....	40
Figure 9: Pigment extraction.....	42
Figure 10: Distribution of elemental composition product and high heating value (HHV) obtained from hydrothermal liquefaction of <i>Nitzschia reversa</i> at different temperatures (error bar presents standard error where n =2).....	44
Figure 11: Biocrude samples obtained from hydrothermal liquefaction of <i>Nitzschia reversa</i> at different temperatures .....	49
Figure 12: Distribution of various product obtained from hydrothermal liquefaction of <i>Nitzschia reversa</i> at different temperatures (error bar presents standard error where n =2).....	51
Figure 13: Distribution of elemental composition (C, H, N, and O) product and high heating value (HHV) in biocrude samples obtained from hydrothermal liquefaction of	

<i>Nitzschia reversa</i> at different temperatures (error bar presents standard error where n =2).....	55
Figure 14: Distribution of organic compounds in biocrude samples obtained from hydrothermal liquefaction of <i>Nitzschia reversa</i> at different temperatures .....	58
Figure 15: Energy recovery on investment (EROI) and energy recovery (ER) values of biocrude production from <i>Nitzschia reversa</i> by hydrothermal liquefaction at different temperature ( error bar represents standard error, where n =2 ) .....	60

## LIST OF EQUATIONS

Equation	1:	%	proteins	=
Absorbance – InterceptslopSample weight (mg)total hydrolysate (mL) x 100.27				
Equation	2:	%	carbohydrates	=
Absorbance – InterceptslopSample weight (mg)total hydrolysate (mL) x 100.28				
Equation 3: % ash content = $\frac{Initial\ weight - Initial\ weight}{Initial\ weight} \times 100$				
.....28				
Equation 4: Higher Heating value (MJ/kg) = $0.338 C + 1.428 (H - 08) + 0.095 S$ .30				
Equation 5: (ER %) = Biocrude yield (%) x biocrude HHV biomass HHV .....31				
Equation 6: (EROI) = Energy outputEnergy input .....31				
Equation 7: Energy output = HHV (biocrude) x biocrude yield.....31				
Equation 8: Energy input = $Q_f + Q_w$ .....31				

## CHAPTER 1: INTRODUCTION

Securing a future energy source and alleviating the impacts of existing energy sources is a necessity (Cheng & Timilsina, 2011). Microalgae are considered to be an energy dense substitution to conventional fuels, and investigations have revealed promising results, while diatoms are known to produce a fine strain that has the ability to produce valuable lipid products and is able to provide a feedstock for biocrude (Shuba & Kifle, 2018). Diatoms have also shown competitive capabilities compared to various algae strains when cultured under favorable conditions, as they can double their biomass faster, where most of the resultant biomass can be utilized efficiently. Diatoms exhibit various types of lipids, free-fatty acids and triglycerides which can be of economic use (Wang & Seibert, 2017). They considered as leading candidate in producing biocrude, while these are the main reasons behind the choices in this study, we also aim to answer if diatoms are able to produce sufficient biocrude when cultured under natural conditions, which was achieved through various objectives and aims, which were, first, isolating the candidate diatom species from Qatari coastal waters. Second, performing molecular analysis and establishing morphological characteristics to identify and characterize the candidate diatom species. Third, carry out a screening of different diatom species under controlled conditions to test their growth attributes using a growth curve. Finally, preceding the selection of a candidate diatom species, performing analysis to investigate the biomass and biocrude production of the candidate diatom under natural conditions.

## CHAPTER 2: LITERATURE REVIEWS

Day after day, the growth of the human population increases rapidly, leading to an expansion in the global industrialization, which depends on fossil fuels mainly for energy production. Indicators illustrate that 90 % of global energy is fossil fuel-based (Galadima & Muraza, 2018). A research pointed out that the consumption rate of crude oil is 105 times higher than what nature can support (Shuba & Kifle, 2018). The continuous exhaustion of non-renewable energy is creating a future shortage, making it harder to meet the future need and demand for energy. The overreliance on fossil fuels resulted in numerous drawbacks such as global warming, ecosystem degradation, environmental and health issues correlated to climate change (Kazemi Shariat Panahi et al., 2019). Thereby, there is an urgent need for alternative energy sources, which must be sustainable, accessible, available, and efficient. Thus, the exploration for renewable, and sustainable energy sources has begun in the past few decades. Different types of renewable energies were investigated and implemented, including solar, hydroelectric, geothermal, wind, and biofuel (Gollakota et al., 2018; Shuba & Kifle, 2018). Recent studies indicate that biofuels are the strongest candidate among other potential energy sources (Shuba & Kifle, 2018). There are a variety of biofuels, which could be derived from bio-based feedstock using different techniques (Leong et al., 2018). Biofuels are classified into three generations depending on the source of biomass (Leong et al., 2018). While the first and second generation of biofuels were derived from edible oil feedstock, and nonedible oil feedstock, third-generation biofuel is derived or is currently being developed from feedstock that could be produced using non-potable water, waste materials, non-arable land, etc. (Leong et al., 2018). The biofuel industry has been booming for the past couple of years, where different sectors are interested in the third generation of biofuel due to the fact that it

does not compete with the production of feed nor food. Galadima and Muraza, (2018) state that microalgae biomass, as one of the third generation biofuel feedstock, could be a strong candidate to be the fuels of the future due to their efficient characteristics: abundance, distribution pattern, growth potential, sustainability as well as processing feasibility (Galadima & Muraza, 2018).

Microalgae term refers to a diverse group of microscopic unicellular photosynthetic organisms (López Barreiro et al., 2013). Microalgae can grow in diverse environmental conditions, although they are mainly found in an aqueous environments (Ren et al., 2018). Unlike other terrestrial plants, microalgae do not require fertile land, and specific quality water; instead, these organisms could be grown using wastewater (seawater/brackish water), light, carbon source, and some trace amounts of nutrients (López Barreiro et al., 2013). The microalgal biomass contains mainly lipids, carbohydrates, proteins, along with little pigments (Menegazzo & Fonseca, 2019). The components level within the biomass is determined by the kind of species or by their growth medium composition (Menegazzo & Fonseca, 2019). These unicellular organisms possess a simple cellular structure with a high surface to volume body ratio (Mandal & Mallick, 2014). Microalgae and plants share the same mechanism of photosynthesis. However, microalgae have higher biomass productivity, higher photosynthetic efficiency, and faster growth rates than terrestrial plants (Gollakota et al., 2018; López Barreiro et al., 2013; Mathimani & Pugazhendhi, 2019). A study indicated that microalgae could capture solar energy 10-50 times higher than most of the terrestrial planets. (Mandal & Mallick, 2014). Another study illustrated that microalgal species could have high lipid content that can reach to more than 70 % of their dry weight under certain condition (Leong et al., 2018; Meng et al., 2009). Microalgae has the ability to



accumulate more lipid content in comparison to terrestrial plants. Microalgal oil could yield over 58,700 to 136,900 l/ha yr, which is 10 to 20 times more than the most efficient oil-producing terrestrial plant (Mandal & Mallick, 2014). Microalgal biofuel has several advantages like the prompt growth, reproduction, and potential of CO<sub>2</sub> mitigation at a rate of 1.83 kg / CO<sub>2</sub> kg<sub>DW</sub> (Shuba & Kifle, 2018). Microalgae also contribute to the reduction of hydrocarbons, particulate matter levels along with the elimination of SO<sub>x</sub> emissions (Shuba & Kifle, 2018). Not only the cultivation of microalgae could reduce the greenhouse gas emission but also microalgae could assist in efficient wastewater bioremediation by utilizing the nutrients as a food source in municipal wastewater treatment (Mathimani et al., 2019). Furthermore, microalgal biomass could be processed further into different valuable products like biomethane, bio-oil, bioethanol, biohydrogen (Leong et al., 2018). Although microalgae are indeed considered to be the favorable organisms to utilize in the production of biofuel, yet the microalgal biomass processing techniques are not commercially exploited yet, and ongoing research activities are addressing some of the challenges. Moreover, their metabolic pathways are not fully understood yet. Therefore, further effort and research is needed for developing sustainable microalgal biofuel.

Among microalgae, Bacillariophyceae have earned interest in their capacity to produce biofuel. Bacillariophyceae are also termed diatoms, which are unicellular photosynthetic eukaryotes (Athanasakoglou & Kampranis, 2019). Their siliceous shell is what differentiates them from other algae (Athanasakoglou & Kampranis, 2019). Diatoms are considered to be the most abundant and significant primary producer species of the ocean, as they are responsible for 40 % of the ocean's primary productivity (Athanasakoglou & Kampranis, 2019). They are one of the most diverse phytoplanktons, including about 100,000 species and more than 200 genera occupying

almost all aquatic environments (Athanasakoglou & Kampranis, 2019; Wang & Seibert, 2017). Diatoms can fix up to 20 % of the global CO<sub>2</sub>; consequently, they significantly contribute in mitigating damages done to the ecosystem (Zulu et al., 2018). The carbon fixed within the diatom is stored as carbohydrates like chrysolaminarin or as lipids like triacylglycerols (TAGs) (Zulu et al., 2018). Diatoms with a wide variety of lipids consist of membrane-bound polar lipids, phospholipid triglyceride, and free fatty acid, together with sterols, waxes, and acyl lipids (Wang & Seibert, 2017). Lipids, especially triacylglycerides (TAGs), are considered to be the primary carbon storage in diatoms and these molecules together could make up to 25 % of the dry biomass (Levitan et al., 2014). Fucoxanthin and didinoxanthin are pigments within the diatoms that have been widely explored in feed, food, cosmeceutical, and pharmaceutical applications (Zulu et al., 2018). Diatoms are incredibly ecologically successful; due to their resilience against pathogens (Levitan et al., 2014). Based on diatoms' lipid profile and physiological characteristics, it has been proven that diatoms are considered to be an excellent target species for producing biofuel feedstock. Diatom growth rates, carbon storage, environmental contribution, and sedimentation rates, and reduced harvesting cost, makes them an ideal candidate with great potential in the biofuel industry (Vella et al., 2019)

Diatoms originate from a complicated evolutionary history; they are considered to be a product of secondary endosymbiosis, which consisted of both green and red algae coupling with a host of the eukaryotic heterotrophic cell (Bowler & Falciatore, 2014). The biomass of diatoms is considered to be a significant contributor to fossil fuels (Bowler & Falciatore, 2014). Athanasakoglou et al. (2017) noted that the distinctive characteristic of diatoms arises from their unique evolution. Diatoms are the result of heterokont lineage that developed by secondary endosymbiosis, that

occurred when a heterotrophic eukaryote has engulfed a red and green algal related cell (Athanasakoglou & Kampranis, 2019). This fusion has grown to be a multi-sourced genetic base, that equipped the diatoms with a complicated yet flexible metabolism, and a wide variety of metabolites (Athanasakoglou & Kampranis, 2019). This class of metabolites is considered to be commercially beneficial with multiple applications in different sectors particularly in the pharmaceuticals, cosmetics, feed, and fuel. An exemplar application is the production of anticancer drugs and antimalarial agents (Athanasakoglou & Kampranis, 2019). About 150 million years ago diatoms joined the record of fossils (Levitan et al., 2014). Their ecological success influenced marine food webs by introducing an organic carbon source (Levitan et al., 2014). Since seventy years ago, geochemists believed that algal lipids are considered to be an essential petroleum feedstock. As a significant fraction of diatoms sinks downward to continental margins and shallow seas, which are then converted to petroleum (Levitan et al., 2014). The origin of algae in the petroleum reservoirs can be traced using lipid analysis as biomarkers (Levitan et al., 2014). Diatom's main biomarkers in the petroleum reservoir are the ratio of steranes, including 28 and 29 carbon atoms, 24-norcholestanes, and highly branched isoprenoid (HBI) alkenes. According to Levitan et al. (2014), these types of biomarkers are detected in various of the topmost quality oil fields worldwide.

*Amphora sp.* is known to be a benthic marine diatom. Several *Amphora* species were mentioned in the literature for their fast growth rate and rich nutritional value (Dias et al., 2018). An research was completed by Chtourou et al. (2015) to investigate the potential of converting *Amphora sp.* and *Navicula sp.* lipids to biodiesel. *Navicula sp.* fatty acid methyl esters (FAME) profile showed the suitability of both diatoms to generate biodiesel (Chtourou et al., 2015). The dominant fatty acids obtained from

FAME profile are palmitic acid, myristic acid, palmitoleic acid, and eicosapentaenoic acid, which are broadly used in the nutrition industry (Chtourou et al., 2015). Furthermore, the influence of the medium composition on the lipid accumulation and growth of *Amphora sp.* was studied, where the biomass of the microalgae was optimized by applying various stressful culture conditions (Chtourou et al., 2015). And the element that illustrated significance in this study was phosphorus (Chtourou et al., 2015). The study concluded that phosphorus deficiency led to the maximum lipid accumulation of 530 mg/g DW, besides the saturated fatty acid (SFAs) were 64.34 % of these accumulated lipids (Chtourou et al., 2015). This study suggested that *Amphora sp.* is capable of being used as biodiesel feedstock (Chtourou et al., 2015). On the other hand, *Amphora subtropica* was isolated from a saline environment to analyze its biomass accumulation under various controlled environmental conditions (BenMoussa-Dahmen et al., 2016). The parameters used to optimize the growth of *Amphora subtropica* were pH, periodicity, temperature, and salinity (BenMoussa-Dahmen et al., 2016). *Amphora subtropica* optimum growth was obtained at a pH of 9 with a 21 h light period and a temperature of 31 °C (BenMoussa-Dahmen et al., 2016). The results revealed that the lipid content increased when the salinity increased from 1 M to 2 M (BenMoussa-Dahmen et al., 2016). With further investigation to improve the fatty acids profile of *Amphora subtropica*, this kind of diatom can be considered as a candidate in the biofuel industry (BenMoussa-Dahmen et al., 2016). Rajaram et al. (2018) demonstrated consistent evidence with the previous study, suggesting that the type of medium highly affects the lipid content formed within the diatom, at which the suitability of *Amphora coffeaeformis* as a biofuel producer was explored, where *Amphora coffeaeformis* was cultured in two different mediums CFTRI-RRAC I and F/2 (Rajaram et al., 2018). The results revealed that the

diatoms cultured in CFTRI-RRAC I medium accumulated more lipid content in comparison to the diatoms cultured in the F/2 medium (Rajaram et al., 2018). Where on the 15th day, when *Amphora coffeaeformis* was cultured in CFTRI-RRAC medium; it exhibited  $149 \text{ mg L}^{-1}$  of lipid fraction while *Amphora coffeaeformis* that was cultured in F/2 medium had  $145 \text{ mg L}^{-1}$  of lipid fraction (Rajaram et al., 2018). The biocrude energy value derived from the hydrothermal liquefaction (HTL) of *Amphora coffeaeformis* biomass cultured in CFTRI-RRAC medium and F/2 medium are 36.19 and 31.70 MJ, respectively (Rajaram et al., 2018). The results indicate that this diatom is a suitable candidate to be considered for biocrude production (Rajaram et al., 2018). Moreover, the fatty acid composition of FAME obtained from microalgae lipid showed that *Amphora coffeaeformis* is suitable for biofuel production (Rajaram et al., 2018). Within these diatoms, *Amphora sp.*, *Nitzschia alexandrina*, and *Nitzschia sp.* were investigated as potential candidates. Where the lipid content for *Amphora sp.* was found to be 19 % DW, while *Nitzschia alexandrinus*' was 13 % DW. Moreover, *Nitzschia sp* showed a lipid content of 30.51 % DW, which is considered to be the highest lipid content among the three. All three Diatoms presented impressive capabilities that can be investigated for further analysis (Cointet et al., 2019).

A study was done in the southern region of the United States to examine the effect of seasonal changes on the rate of the growth, proteins, lipids, and fatty acid profile of *Nitzschia sp.*. The diatom was cultured under three laboratory cycles which were created to represent the following seasons; summer, spring/fall, and winter. The study also aimed to inspect the diatoms' growth under five different concentrations of silica (Jiang et al., 2014). The results showed that the summer season produced the highest biomass; however, winter season cultured diatoms produced the optimum

lipid content (Jiang et al., 2014). Furthermore, the diatoms that grew under higher silica concentrations had a high rate of growth in summer and spring/fall season with low organic content (Jiang et al., 2014). Nonetheless, diatoms that grew under silica deficient mediums had higher neutral lipid level (Jiang et al., 2014). During summer condition, SFAs and monounsaturated fatty acids (MUFAs) were more constant than both spring-fall and winter seasons (Jiang et al., 2014). The content of polyunsaturated fatty acids (PUFAs) in summer were remarkably low. In the winter season, SFAs and MUFAs were decreased gradually while PUFAs increased slowly with the increased concentrations of silica (Jiang et al., 2014). Generally the seasonal conditions affect the composition of fatty acid (Jiang et al., 2014). The study concluded that high silica concentration increased the biomass productivity of *Nitzschia sp.* in all seasonal conditions (Jiang et al., 2014). On the other hand, silica deficiency increased the lipid content within *Nitzschia sp.* in all seasonal conditions (Jiang et al., 2014). The conflict between maximizing biomass yield and lipid accumulation require further studies for overall lipid productivity (Jiang et al., 2014). A study was performed by Sahin et al. (2019) to examine the impact of varied nitrogen and iron content on the growth, fucoxanthin, lipid content, and fatty acids profile of *Nitzschia sp.*; the findings of the study are presented in Table 1.

Table 1: Cell density, growth rate, biomass, lipid content, and fucoxanthin content of marine diatoms cultivated under different mediums.

	Nitrogen rich medium	Iron-rich medium
Cell density	$55.9 \times 10^4$ cells mL <sup>-1</sup>	$51.67 \times 10^4$ cells mL <sup>-1</sup>
Growth rate	0.313 day <sup>-1</sup>	0.294 day <sup>-1</sup>
Biomass	2.66 g L <sup>-1</sup>	868 g L <sup>-1</sup>

Lipid content	21.62 %	37.03 %
Fucoxanthin content	7.83 mg g <sup>-1</sup> DW	6.16 mg g <sup>-1</sup> DW

---

Table 1 showed that the *Nitzschia sp.*, cultivated in nitrogen rich medium, showed a rapid growth with a maximum cell density of  $55.9 \times 10^4$  cells mL<sup>-1</sup> along with a specific growth rate of 0.313 per day (Sahin et al., 2019). Additionally, *Nitzschia sp.* obtained the maximum biomass of 2.66 g L<sup>-1</sup> when it was grown in nitrogen rich medium (2 g L<sup>-1</sup> of NaNO<sub>3</sub>). *Nitzschia sp.* cultured in the nitrogen free medium presented higher lipid content of 37.03 % compared to lipid the content of *Nitzschia sp.* grown in nitrogen rich medium, which was 21.62 % (Sahin et al., 2019). The diatoms cultivated in N-rich medium produce the maximum fucoxanthin fraction of 7.83 mg g<sup>-1</sup> DW (Sahin et al., 2019). The major fatty acids obtained from *Nitzschia sp.* lipid profile were palmitic acid (C16:0), stearic acid (C18:0), palmitoleic acid (C16:1) and oleic acid (C18:1n9c). However, the composition of saturated and unsaturated fatty acids varied under nutrient-stress conditions. The produced fatty acids under nutrient-stress conditions constituted of up to 90% of saturated and unsaturated fatty acids, which gave *Nitzschia sp.* the potential to produce biodiesel (Sahin et al., 2019). While microalgal lipid could be converted to biodiesel, whole biomass of microalgae could be processed to produce biocrude oil using Hydrothermal liquefaction (HTL). The HTL process is the conversion of biomass into liquid biocrude in the presence of hot compressed water (Mohan et al., 2013).

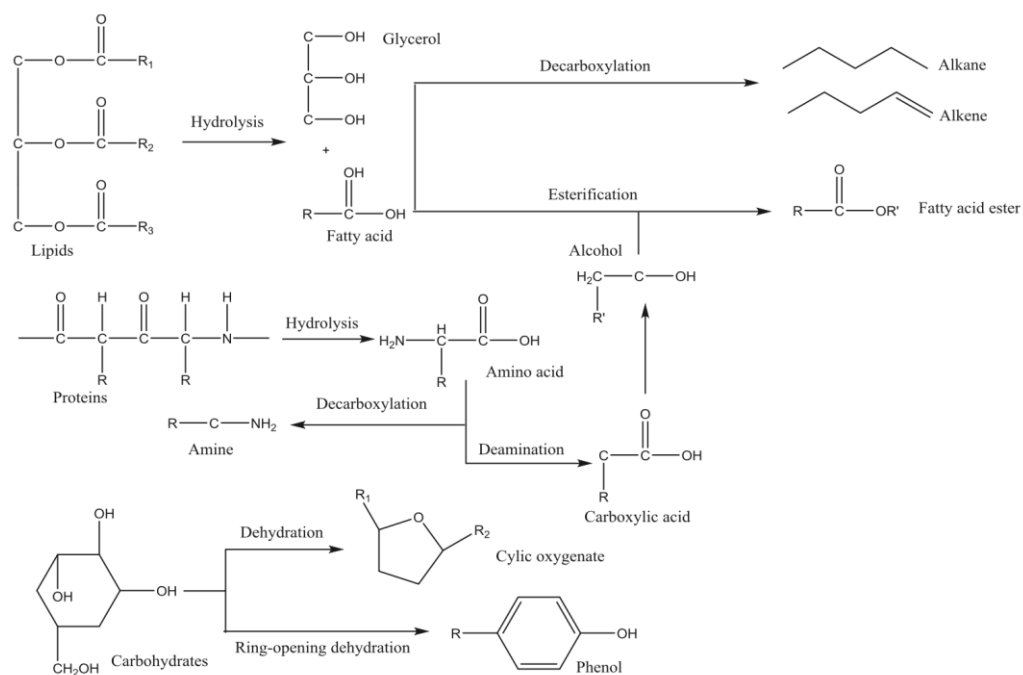


Figure 1: An overall reaction mechanism for HTL of microalgae

Figure 1 illustrated that conversion of microalgae to biocrude during HTL comprises of conversion reactions of three major components: Lipid, protein and carbohydrates (Yulin Hu et al., 2019). Triglyceride is the major form of lipids found in microalgae, at which it is easily broken down through the process of hydrolysis into glycerol (oily phase) and free fatty acids, except when broken down under high heat, the glycerol exists in water phase (Yulin Hu et al., 2019). Fatty acids are considered to be highly stable in water but can sometimes be decomposed to form long hydrocarbon chains (Yulin Hu et al., 2019). The second major component is the protein, which is comprised of polymers of amino acids linked by peptide chains, these polymers can be broken down into simpler amino acids when exposed to high temperature (Yulin Hu et al., 2019). Where these amino acids undergo two decomposition pathways: decarboxylation and deamination, where both usually occur in hydrothermal conditions (Yulin Hu et al., 2019). Carbohydrates are found in



microalgae in various known forms: starch, cellulose and other polysaccharides(Yulin Hu et al., 2019). Cellulose is a crucial component which forms the microalgal cell wall, which is an insoluble molecule in water, unless it is subjected to near critical water at which it will be hydrolyzed to glucose monomers (Yulin Hu et al., 2019). Hemicellulose is another form of carbohydrates found in microalgae, at which it is less resistant to degradation under high temperatures(Yulin Hu et al., 2019). On the other hand, starch can also be readily degraded under hydrothermal conditions (Yulin Hu et al., 2019). A study proposed that HTL could produce up to 38 to 64 wt % of biomass into biocrude, which could be composed of 50–80 % carbon, 5 to 18 wt % oxygen, 4 to 8 wt % nitrogen. The produced biocrude could have a high viscosity of 40 to 67 cP, total acidity number of 25 – 118 mg KOH/g, and higher heating value (HHV) of 25 to 37 MJ/ kg (Kazemi Shariat Panahi et al., 2019). Hydrothermal liquefaction of biocrude oils comprise of different types of chemical compounds in particular straight and branched aliphatic compounds, aromatics and phenolic derivatives, esters, nitrogenous ring structures and carboxylic acids (Vardon et al., 2011). The type of these compounds is affected by the portions of protein, lipids, and carbohydrates within the microalgal biomass (Vardon et al., 2011). Likewise, the reaction parameters of hydrothermal liquefaction such as reaction interval time, temperature, and biomass to water ratio impact the composition of biocrude oil (López Barreiro et al., 2018).

Biocrude is usually identified by high heteroatom contents, mainly in the form of oxygenated and nitrogenous compounds (Vardon et al., 2011). The content of heteroatom is the main distinctive factor that differentiate biocrude from crude petroleum (Vardon et al., 2011). High heteroatom content creates unfavorable properties such as oil acidity, polymerization, high viscosity, and high-boiling

distribution (Vardon et al., 2011). Besides, the biocrude chemical composition has a strong influence on combustion performance, upgrading response, storage stability, and commercial value (Vardon et al., 2011). The advantage of the (HTL) process in comparison with other processes is that the entire microalgal biomass can be used for biocrude production (Kazemi Shariat Panahi et al., 2019). Besides, it's more efficient as it does not require dried microalgal biomass because the moisture within the biomass acts as a reaction medium, where total biomass is decomposed and converted in hot compressed water (Kazemi Shariat Panahi et al., 2019; López Barreiro et al., 2018; Tian et al., 2014). The process of conversion is not limited to lipid content only, protein content and carbohydrate content are also converted to biocrude. Therefore, lipid content is not the critical component in hydrothermal liquefaction (HTL) because HTL has the ability to convert the entire microalgal biomass. A study concluded that algae biomass with 0.1 % of lipids were able to produce a biocrude yield of 39.0 % through HTL (Tian et al., 2014). Another research indicated that the biocrude yield could increase up to 15 % higher than the lipid content of the microalgae biomass (Biller & Ross, 2011). Furthermore, the produced biocrude is characterized by low oxygen content, and high calorific value. Further, low level of sulfur and particulate matter (ash) were released in the process of biocrude combustion (López Barreiro et al., 2013; Shuba & Kifle, 2018). Additionally, the chemical composition of the microalgae affects the quality of biocrude yield (Kazemi Shariat Panahi et al., 2019). Biocrude can be used as a promising alternative for petro-crude in the petroleum refinery. However, there are still major challenges in the process of hydrothermal liquefaction (HTL) such as uncomprehensive knowledge of the reaction chemistry and kinetics, proper catalysts, management of by-products, fouling and plugging. Another drawback is the high NO<sub>x</sub> emission coming from the high nitrogen content

within the microalgae's chlorophyll and proteins (López Barreiro et al., 2013; Shuba & Kifle, 2018). Further refineries are needed in some cases of high viscosity, high heteroatoms (primarily O and N) and presence of carboxylic acids (Li & Savage, 2013). These treatments of hydrothermal liquefaction biocrude can be complicated and costly; hence more studies are required to screen other microalgal biomass feedstock that could minimize these problems. (Li & Savage, 2013).

Hydrothermal liquefaction is usually operated at a high temperature and high pressure. A various number of microalgal strains have been investigated as feedstocks for HTL conversion to biocrude. Table 2 demonstrates microalgal strains that were successfully converted into biocrude by HTL, which include *Nannochloropsis sp.*, *Tetraselmis sp.*, and *C. vulgaris* (Eboibi et al., 2014; He et al., 2020). Comparison of microalgal biocrude yield in Table 2 showed that HTL temperature is a critical factor affecting the biocrude yield. Furthermore, the type of microalgal species can influence the biocrude yield as each specie has a different chemical composition that impacts the resulting HTL biocrude (Biller & Ross, 2011).

Table 2: An overview of studies investigating biocrude yield produced from microalgal HTL

Species name	HTL temperature	HTL time	Biocrude yield %	Reference
<i>Nannochloropsis sp.</i>	260 °C	20 min	39.05	(He et al., 2020)
<i>Nannochloropsis sp.</i>	280 °C	20 min	43.55	(He et al., 2020)
<i>Nannochloropsis sp.</i>	300 °C	20 min	45.35	(He et al., 2020)
<i>Nannochloropsis sp.</i>	320 °C	20 min	54.11	(He et al., 2020)
<i>Nannochloropsis sp.</i>	340°C	20 min	41.73	(He et al., 2020)

<i>Tetraselmis sp</i>	310 °C	30 min	41	(Eboibi et al., 2014)
<i>Tetraselmis sp</i>	330 °C	30 min	60	(Eboibi et al., 2014)
<i>Tetraselmis sp</i>	350 °C	30 min	51	(Eboibi et al., 2014)
<i>C. vulgaris</i>	300 °C	13 min	39.69	(Palomino et al., 2020)
<i>C. vulgaris</i>	350 °C	10 min	42.1	(Palomino et al., 2020)

A study performed by Tzanetis et al. (2017) assessed the techno-economic effect of hydrothermal liquefaction and biocrude upgrading by primarily testing various alteration in significant reaction variables including catalysts, Iron(aq), catalyst biomass ratio, and temperature. Where the effects were assessed using the following simulations: process economics and life cycle greenhouse gases. Where the lowest production cost of biocrude was at (450 €/t<sub>biocrude</sub>) and was obtained at HTL conditions of 340 C with Iron(aq) as a catalyst (Tzanetis et al., 2017). However, the price would increase after hydrotreatment and fractionation, to 1086 €/t<sub>biojet-fuel</sub>, which is more than the commercial value of fossil jet fuel. Tzanetis et. (2017) believes that investing in optimization processes will lead to a successful economic equation.

## CHAPTER 3: MATERIALS AND METHODOLOGY

### Materials

#### *Media preparations*

For F/2 nutrient medium preparation, the following components shown in Table 3 were added to 950 mL of filtered natural seawater. The vitamins and silica were added after the mixture is autoclaved. Then the final volume is brought up to 1 liter by filtered seawater.

Table 3: Composition of F/2 growth medium.

Component	Stock solution	Quantity	Molar concentration in final medium
NaNO <sub>3</sub>	75 g/L dH <sub>2</sub> O	1 mL	8.82 x 10 <sup>-4</sup> M
NaH <sub>2</sub> PO <sub>4</sub> H <sub>2</sub> O	5 g/L dH <sub>2</sub> O	1 mL	3.62 x 10 <sup>-5</sup> M
Na <sub>2</sub> SiO <sub>3</sub> 9H <sub>2</sub> O	30 g/L dH <sub>2</sub> O	1 mL	1.06 x 10 <sup>-4</sup> M
trace metal solution	(Table 4)	1 mL	***
vitamin solution	(Table 5)	0.5 mL	***

For trace metal solution, the following components presented in Table 4 were added to 950 mL of dH<sub>2</sub>O. The final volume is brought up to 1 liter by dH<sub>2</sub>O and autoclaved.

Table 4: F/2 Trace metal solution

Component	Primary solution	stock	Quantity	Molar concentration in final medium
FeCl <sub>3</sub> 6H <sub>2</sub> O	***		3.15 g	1.17 x 10 <sup>-5</sup> M
Na <sub>2</sub> EDTA 2H <sub>2</sub> O	***		4.36 g	1.17 x 10 <sup>-5</sup> M
CuSO <sub>4</sub> 5H <sub>2</sub> O	9.8 g/L dH <sub>2</sub> O		1 mL	3.93 x 10 <sup>-8</sup> M
Na <sub>2</sub> MoO <sub>4</sub> 2H <sub>2</sub> O	6.3 g/L dH <sub>2</sub> O		1 mL	2.60 x 10 <sup>-8</sup> M
ZnSO <sub>4</sub> 7H <sub>2</sub> O	22.0 g/L dH <sub>2</sub> O		1 mL	7.65 x 10 <sup>-8</sup> M
CoCl <sub>2</sub> 6H <sub>2</sub> O	10.0 g/L dH <sub>2</sub> O		1 mL	4.20 x 10 <sup>-8</sup> M
MnCl <sub>2</sub> 4H <sub>2</sub> O	180.0 g/L dH <sub>2</sub> O		1 mL	9.10 x 10 <sup>-7</sup> M

For vitamins solution, the following components presented in Table 5 were added to 950 mL of dH<sub>2</sub>O. Thiamine was dissolved, and 1 mL of the primary stocks were added. Then by dH<sub>2</sub>O the final volume is brought up to 1 liter.

Table 5: Vitamin Solution

Component	Primary Solution	Stock	Quantity	Molar Concentration in Final Medium
thiamine	***		200 mg	2.96 x 10 <sup>-7</sup> M
biotin	1.0 g/L dH <sub>2</sub> O		1 mL	2.05 x 10 <sup>-9</sup> M
cyanocobalamin	1.0 g/L dH <sub>2</sub> O		1 mL	3.69 x 10 <sup>-10</sup> M

### *Solutions and reagents*

#### Vanillin phosphoric acid reagent:

Vanillin phosphoric acid reagent (VSP) was prepared by dissolving 0.12 g of P-vanillin in 2 mL absolute ethanol. 18 mL of deionized water and 80 mL of phosphoric acid were added to the sample.

#### Lowry Solution:

Lowry Solution was made by mixing solutions X, Y, and Z with a ration of (10:0.1:0.1) identified as the following: solution X is prepared by dissolving 2.8598 g of sodium Hydroxide (NaOH) and 14.3084 g of sodium carbonate of ( $\text{Na}_2\text{CO}_3$ ) in 500 mL of deionized water. For solution Y 1.4232 g of copper sulfate ( $\text{CuSO}_4 \cdot 5\text{H}_2\text{O}$ ) dissolved in 100mL of deionized water. Solution Z is prepared by dissolving 2.85299 g of sodium tartrate ( $\text{C}_4\text{H}_4\text{O}_6\text{Na}_2$ ) in 100 mL of deionized water.

#### The Folin Reagent:

5 mL of 2N Folin and Ciocalteu's phenol reagent are dissolved in 6 mL of deionized water.

#### D-Glucose standard solution:

D-Glucose standard solution is obtained by dissolving 0.3 g D-glucose was dissolved in 100 mL deionized water.

#### Phenol-sulfuric reagent:

15 mL of sulfuric acid was added to 7.5 mL of deionized water. After the solution cooled down, 0.15 g phenol crystals were added to the solution.

### *Kits*

GenElute™ Plant Genomic DNA Miniprep kit (Sigma, USA)

Minielute Gel Extraction kit (Qiagen, USA)

## **Methods :**

### ***Collection***

One liter of seawater, mixed with seagrass, was collected in wide-mouthed 500 mL sample bottles. The collection of the samples was performed within the area of Al-Mafjar intertidal zone (26°09'39.2"N 51°15'03.6"E ).

### ***Isolation and purification of the diatom strains performed as it described in (Robert A. Andersen, 2005)***

Steps preceding water sampling involved graded filtering, where the sample was passed successively through two filters, with 40 microns, and 20-micron pores respectively. Two to five drops of filtered seawater are placed on a concaved slide for observation and identification under light-microscopy (Primo Star HAL Microscope, full Köhler, stage drive R, FOV 20, Carl Zeiss, Germany). Later on, morphological identification, isolation methods were implemented for the removal of unwanted microorganisms. Isolation of diatom strains was conducted by serial dilution and single-cell isolation that has been applied in parallel to obtain pure cultures. The single-cell isolation technique was performed by picking up single cells of the desired species using micropipette handled under a microscope. Then the species were carefully transferred onto a new concave slide that contained 2-4 drops of F/2 media. Serial dilution was applied and observed under the microscope to remove organic debris, zooplankton, and other contaminants until the sample was clean and pure. The above processes were repeated several times until a single cell of the desired diatom species was isolated. The isolated diatom species is classified initially at the morphological level by light microscopy (40×, Primo Star HAL Microscope, full Köhler, stage drive R, FOV 20, Carl Zeiss, Germany). The isolated strain was



transferred to 10 mL F/2 media to be kept as a pure culture. Strain stock culture was incubated in growth chamber (Sanyo, Japan) at 28 °C, a photon flux density of 100 mol photons m<sup>-2</sup> s<sup>-1</sup> and a 12:12 h dark:light cycle.

### ***Screening of diatom strains***

Preliminary screening was performed mainly to examine the candidate diatom species, by testing their survival potential in an F/2 medium, where a total of three strains *Nitzschia reversa*, *Trachyneis aspera* and *Amphora sp.* were taken for prescreening and examined in 24-well MicroWell Plates. The strains were initially inoculated in MicroWell Plates containing 300 µL F/2 culture medium and incubated in growth chamber (Sanyo, Japan) at 28 °C, a photon flux density of 100 mol photons m<sup>-2</sup> s<sup>-1</sup> and a 12:12 h dark:light cycle for a period of 1 week (Robert A. Andersen, 2005). The survival of the diatom strains were examined under the microscope.

Final screening criteria depended on the survival potential of the previously inoculated strains, where the survived strains in the F/2 culture medium were subjected to the final screening, at which only one was chosen to be the candidate for biocrude production. During the final screening, optimization of salinity levels, nitrogen source, and nitrogen concentration on diatom growth was performed as described in the following sections.

### ***Optimization of salinity levels on diatom growth***

The diatom strains were grown in 40 ppt, 50 ppt, and 60 ppt salinity cultures so that optimum culture salinity could be determined for these two strains. The diatom strains were cultured in 50 mL F/2 medium contained in stoppered 6 Erlenmeyer flasks for each strain. Ten percent (5 mL) of each strain was inoculated into 250 mL Erlenmeyer flask containing 45 mL of F/2 medium with 3 different salinities. All these treatments were carried out in duplicates. The cultures were placed in an orbital shaker

at 150 rpm, 30 °C, photon flux density of 100 mol photons m<sup>-2</sup> s<sup>-1</sup> and a 12:12 h dark:light cycle using Innova® 44R incubator shaker (New Brunswick Scientific, USA) for 15 days. Growth of these strains was measured by UV/visible spectrophotometer through optical density (OD 750 nm,) every other day.

### ***Optimization of nitrogen source on diatom growth***

To obtain a suitable nitrogen source for diatom's optimum growth, diatom strains were grown also in F/2 medium under optimized salinity from the previous experiments with an alternative source of nitrogen for each treatment. Three nitrogen sources, e.g., sodium nitrate (NaNO<sub>3</sub>), Ammonium chloride (NH<sub>4</sub>Cl), and Urea (CH<sub>4</sub>N<sub>2</sub>O) were examined. All the nitrogen sources were added to DI water, such that each of the solution contained a nitrogen concentration that was equivalent to the nitrogen concentration in the standard F/2 medium. The standard F/2 medium contains 75 g of NaNO<sub>3</sub>/ L of which has 14.0067 g nitrogen. Each treatment consisted of the same concentration of nitrogen. The diatom strains were cultured in 50 mL of F/2 medium contained in stoppered 6 Erlenmeyer flasks for each strain. Ten percent (5 mL) of each strain was inoculated into 250 mL Erlenmeyer flask containing 45 mL of F/2 medium consisting of 1 mL of NaH<sub>2</sub>PO<sub>4</sub>·2H<sub>2</sub>O, 1 mL trace metal solution, 1 mL silica, 1 mL F/2 vitamin, and 2 mL of nitrogen source. All treatments were carried out in duplicate. The cultures were incubated at 150 rpm, 30°C, photon flux density of 100 mol photons m<sup>-2</sup> s<sup>-1</sup> and a 12:12 h dark:light cycle using Innova® 44R incubator shaker for 15 days. The growth of these strains was measured by UV/visible spectrophotometer through optical density (OD 750 nm) every other day.

### ***Optimization of nitrogen concentration on diatom growth***

After obtaining the optimal nitrogen source, different concentrations of optimized nitrogen sources were tested (14, 28, and 42 mg N/L ). The diatom strains

were then cultured in 50 mL of F/2 medium contained in stoppered 6 Erlenmeyer flasks for each strain. Ten percent (5 mL) of each strain was inoculated into 250 mL Erlenmeyer flask containing 45 mL of F/2 medium. The cultures were incubated at 150 rpm, 30 °C, photon flux density of 100 mol photons m<sup>-2</sup> s<sup>-1</sup>, and a 12:12 h dark:light cycle in an Innova® 44R incubator shaker for 15 days. The growth of these strains were measured by UV/visible spectrophotometer through optical density (OD 750 nm) every other day.

### ***Pre-cultivation of inoculum in indoor systems***

The selected diatom was initially inoculated in 250-mL Erlenmeyer flasks containing 50 mL 3x F/2 culture medium. Flasks were placed on a shaker at 150 rpm, 30°C, photon flux density of 100 mol photons m<sup>-2</sup> s<sup>-1</sup> and a 12:12 h dark:light cycle using Innova® 44R incubator shaker for 15 days. The inoculum was then transferred to 500 mL Erlenmeyer flasks containing 250 mL 3x F/2 culture medium and incubated in the shaker with similar conditions for 15 days (BenMoussa-Dahmen et al., 2016). Next, the inoculum was transferred to 1000 mL Erlenmeyer flasks containing 500 mL 3x F/2 culture medium and placed in the shaker with the same conditions for 15 days. In the proceeding step, the inoculums were transferred to 2000-mL Erlenmeyer flasks containing 1000 mL 3x F/2 culture medium and placed in the shaker in similar conditions for 15 days. This culture was used to divide and transfer equally to two 2000 mL Erlenmeyer flasks containing 1000 mL 3x F/2 culture medium and placed in the shaker in similar conditions for 15 days. At the last stage of inoculum preparation, 2 L culture from the previous step was transferred to 10 L plastic photobioreactors (PBR) containing 8 L 3x F/2 culture medium and cultivated in an indoor cultivation system. The PBR received 600 µmol E/m<sup>2</sup>/s light intensity for a 12:12 h dark:light cycle obtained by means of white fluorescent tube-lights; the

culture was mixed by air, supplied by an air compressor, at a rate 0.5 L/min (P. Das et al., 2019)

### ***Mass cultivation of inoculum in open pond system***

The mass cultivation was held in 5 sq. m open raceway pond at Zubrah area, in the north of Qatar. The 4 m × 1.25 m raceway pond made from fiberglass. The raceway tank is kept on a concrete base above the ground facing the direction of North-South (Probir Das et al., 2019). One day before the inoculation, 500 L of seawater was first passed through 4.4 C Aquadyne filter and then sterilized with 0.02% (v/v) commercial grade bleach ; afterwards, it was added to the raceway tank. Later, 50 L of microalgal culture was inoculated onto the raceway tank. Nutrients were added as per Guillard 3x F/2 protocol (Guillard & Ryther, 1962). A paddlewheel system was connected to an electric AC motor; the shaft of the motor was connected to gear and pulley and the rotation of the paddlewheel was set at 20 rpm giving a liquid flow velocity of 20 cm/s in the raceway tank (Probir Das et al., 2016). 99.99% pure CO<sub>2</sub> was injected at the bottom of the raceway pond with the help of an air-stone. The depth of the ponds was 10 cm and the daily evaporation water loss was regulated at 10 cm by adding freshwater (Probir Das et al., 2016). The duration time of cultivation was 15 days. Samples of the culture were regularly examine under the microscope for possible biological contamination.



Figure 2: Raceway pond

*Microalgae harvesting performed as described by (P. Das et al., 2019)*

In order to obtain a concentrated microalgal biomass, tangential flow filtration (TFF) unit was used as a preliminary harvesting technique. The microalgal stream was pumped from the raceway pond into the 700 L cylindrical feed tank; another pump was connected to the bottom of the feed tank to pump the culture across the TFF membrane. TFF membrane had 1740 hollow fibers made of polyacrylonitrile (PAN) having 10 kDa as a molecular weight cut-off. The length of each hollow fiber was 105 cm with an i.d. of 1 mm. The surface area of the TFF membrane was 25 m<sup>2</sup>, and the maximum operating pressure was 3 bar. The microalgal stream, which passed through a membrane, referred to as the permeate. This permeate contained molecules smaller than the membrane pores, which is the F/2 medium only without the microalgal biomass. Eventually, permeate was carried to a waste tank by a PVC tube. However, the other

portion of the stream having concentrated microalgal culture was referred to as the retentate. The retentate contained the stream of interest, which was the microalgal biomass. The retentate was recirculated back to the feed tank by a PVC tube. This process was continuously repeated until biomass was concentrated to the desired level. The dense retentate was then centrifuged (benchtop Thermo Fisher SL 16 R centrifuge, USA), and then stored directly at  $-20\text{ }^{\circ}\text{C}$ .



Figure 3: Tangential flow filtration (TFF) unit

#### ***Lipid content and fatty acid methyl esters (FAMES)***

Lipid content in the algal biomass was determined by fatty acid methyl esters derivatization and gas chromatograph fitted with a flame ionization detector (GC-FID). The extraction of FAMES was done in duplicates. 15 mg of freeze-dried biomass was added to an adequate volume of sulfuric acid (95%) and methanol ( $\text{H}_2\text{SO}_4:\text{CH}_3\text{OH}$ , 1:10) in a 20 mL glass vial; the cap of the vial had PTFE seal to prevent the leaking of gas. Then, the mixture was sonicated for 10 min in a sonication chamber (Branscon 1510, Mexico). Next, the vial was kept in a furnace for two hours at  $80\text{ }^{\circ}\text{C}$ . Then the

vial was removed from the furnace and kept in an ice bath; the cooled down mixture was then transferred to a centrifuge tube containing 1 mL distilled water and a mixture of hexane:chloroform (4:1). After 5 min of centrifugation at 5000 rpm, the organic layer containing the derivative FAMES fraction was transferred to pre-washed 40 mL glass tube. The weight of the 40 mL glass tube was recorded. The steps from the addition of distilled water and a mixture of hexane: chloroform (4:1) following by centrifugation and organic layer separation were repeated (one/two) more times to collect the organic fraction. The extracted FAMES were analyzed using GC-FID; 2 uL of the sample extract was injected into gas chromatography. The oven temperature program was set at 100 °C and increased at 5 °C/min to 240 °C. The fatty acid methyl esters (FAMES) in the sample were separated using a 100 m column; helium gas was used as a carrier gas. FAME peaks were identified and quantified by comparison to their retention times and peaks area with those of standards, using 37 FAMES supelco standards from marine oil.

***Quantitative analysis of lipids using sulfo-phospho-vanillin as described by  
(Byreddy et al., 2016)***

Lipids content in the microalgal strain was quantified by colorimetric sulfo-phospho-vanillin (SPV) method. First, 10 mg of commercial oil was transferred in tube with 50 mL chloroform. Different volumes of the mixture were transferred to five glass vials (0.05, 0.1, 0.2, 0.3, 0.4 mL). The vials were incubated at 60 °C until chloroform is totally evaporated. Then 0.72 mL of sulfuric acid was added to each glass. After 10 minutes, 1.78 mL of Vanillin-phosphoric acid reagent was added to each glass vial. The absorbance of the samples was measured at a wavelength of 530 nm.

***Quantitative analysis of protein using Lowry method performed as it was described  
by (López et al., 2010)***

Crude protein fraction in the microalgae strain was quantified by the Lowry method. First, to facilitate the extraction of proteins, 5 mL of 0.1 N NaOH, along with glass beads, were added to 25 mg of freeze-dried biomass in the centrifuge tube. The centrifuge tube was vortexed and incubated overnight at 60 °C. The sample was further treated using tissue lyser for 5 min followed by centrifugation and supernatant collection; the process was repeated twice to have a negligible amount of proteins for the Lowry assay, maceration of the pellet using 0.1 N (NaOH) was repeated. Lowry assay started with the addition of 0.7 mL of Lowry solution to 0.5 mL of the lysate (mix) and followed by a light vortex. Then this reaction mixture was incubated in a dark room for 20 minutes and immediately followed by the addition of 0.1 mL of Folin reagent to the sample and was then vortexed. After 30 minutes, a spectrophotometer was used to read the absorbance of the sample at a wavelength of 750 nm. Calibration curve was established with different concentrations (0.01 mg/mL to 10 mg/mL) of bovine serum albumin standard dissolved in 0.1 N NaOH to convert the spectrophotometric absorbance to protein concentration using Equation 1.

$$\text{Equation 1: \% proteins} = \frac{\text{Absorbance} - \text{Intercept}}{\text{slop}} \times \frac{\text{Sample weight (mg)}}{\text{total hydrolysate (mL)}} \times 100$$

***Quantitative analysis of total carbohydrates by phenol-sulfuric acid colorimetric assay performed as it described by (Dubois et al., 1951)***

Phenol-sulfuric acid colorimetric assay was used to measure the carbohydrate concentration in aqueous solutions. 10 mg of freeze-dried biomass was transferred to polypropylene conical centrifuge tube. 2 mL glacial acetic acid was added to the biomass and lightly vortexed. The mixture was placed for 20 min in an 85 °C water bath for 20 min to obtain decolorized biomass. Once the pellet turned colorless, the



sample was removed, and 4.5 mL acetone was added to the mixture and then vortexed. After centrifugation of the mixture at 4000 rpm for 10 mins at 20 °C, the acetone was discharged by removing the supernatant. 5 mL of 4 M HCl was transferred to the decolorized pellet. Then, the sample was vortexed and placed for 2 h into boiling water. Immediately 5 mL of distilled water was transferred to the sample and then centrifuged for 10 min at 4000 rpm at 20 °C. 20 µl of the supernatant was then added to a 2 mL microcentrifuge tube and placed in an ice bath. 90 µl of the phenol-sulfuric acid reagent was transferred to the 2 mL microcentrifuge tube. The mixture was then vortexed and placed for 20 min in a boiling water bath. After allowing the mixture to cool, 300 µl of each mixture was placed into a 96-well microplate. The absorbance of the samples were measured at a wavelength of 490 nm. Calibration curves were established with different concentrations (1.5, 1, 0.5, 0.2, 0.1 mg/mL) of D-glucose standards dissolved in distilled water. The spectrophotometric absorbance was then converted to carbohydrates concentration using Equation 2.

$$\text{Equation 2: \% carbohydrates} = \frac{\text{Absorbance} - \text{Intercept}}{\text{slope}} \times \frac{\text{Sample weight (mg)}}{\text{total hydrolysate (mL)}} \times 100$$

***Ash Content performed as it was described by (Probir Das et al., 2020)***

0.1 g of dry biomass was transferred to a ceramic crucible to be incubated in a muffle furnace for 4 hours at 540 °C. The ash content was determined using

Equation 3.

$$\text{Equation 3: \% ash content} = \frac{\text{Initial weight} - \text{Final weight}}{\text{Initial weight}} \times 100$$

### *Hydrothermal liquefaction experiment*

Hydrothermal liquefaction (HTL) was used to convert *Nitzchia reversa* biomass into biocrude, next to gaseous, aqueous, and solid by-products. HTL was carried out in 10 mL high-pressure Swagelok fitting type reactors. 1 g of *Nitzchia reversa* dried biomass and 6 mL of deionized water was added in the Swagelok reactors, which was then sealed tightly and then placed in a muffle furnace. The HTL experiments were operated at five temperatures ( 300, 325, 350, 375, and 400 °C), and the reaction time for all HTL experiments was 30 minutes. After the reaction was completed, the reactor was exposed to flowing cold water to cool down the Swagelok reactors. Then, the reactor plug was opened carefully to vent out gases to the atmosphere. The reaction mixture was removed from the reactor to a glass tube. 10 mL of dichloromethane was loaded to the reaction mixture to facilitate the formation of the upper layer of the aqueous phase and the bottom layer of the organic phase, which contained the biocrude fraction. The two layers were separated, centrifuged at 5000 rpm for 10 min; afterward, the organic phase layer was analyzed for biocrude yields, quality, and biochar yields.



Figure 4: 10 mL high-pressure Swagelok fitting type reactors

***Biochar content performed as described by (Probir Das et al., 2020)***

The biochar content was determined by placing centrifuged pellets from aqueous and organic phases into ceramic crucible to be incubated in a muffle furnace for 24 hours at 105 °C. The dried biochar was weighed, and the biochar content was determined.

***Quantitative analysis of biocrude***

The biocrude content was determined by placing 2 mL of an organic layer into a glass tube and kept it at 60 °C in a HACH DRB 200 block heater for 10 minutes to evaporate the dichloromethane (Probir Das et al., 2020). Then, the biocrude sample was weighed, and the biocrude content was determined.

***Calorific values and CHNS analysis performed as described by (P. Das et al., 2019)***

The calorific values of both biomass and biocrude samples were determined by using Equation 4. The higher heating value (HHV) was calculated using Dulong's empirical formula. The elemental composition (C, H, and N) of the samples were determined by a Flash 2000 CHN analyzer (ThermoFisher Scientific, USA). Where the oxygen content was determined by deducting the total of C, H, and N content from 100.

$$\text{Equation 4: Higher Heating value (MJ/kg)} = 0.338 C + 1.428 \left( \frac{H-O}{8} \right) + 0.095 S$$

***GC-MS analysis***

The organic compounds in the biocrude were determined by a 7890A Agilent Technologies GC system coupled with a 5973 Network mass selective detector (P. Das et al., 2019). A 1 µL sample (in split-less mode) was injected into the GC column (30 m × 250 µm × 0.25 µm Rxi-5Sil MS column) using helium carrier gas at 15 psi

pressure and a flow velocity of 1.67 mL/min. The temperature of the injector was held constant at 300°C. After the sample was injected, the temperature of the oven was initially held at 60 °C for 2 min, then increased by 6 °C per minute to finally reach 300 °C, which maintained for 20 min. By using an ion source, various compounds in the gas stream were ionized. In MS-scan mode, the mass spectrometer was operated. Different compounds in the biocrude samples were classified using the NIST98 mass spectral library database

**Determining energy recovery and energy return on investment as described by (Liu et al., 2018; Yoo et al., 2015)**

Energy recovery (ER %) and energy return on investment (EROI) were calculated by the following equations:

$$\text{Equation 5: (ER \%)} = \text{Biocrude yield (\%)} \times \frac{\text{biocrude HHV}}{\text{biomass HHV}}$$

$$\text{Equation 6: (EROI)} = \frac{\text{Energy output}}{\text{Energy input}}$$

$$\text{Equation 7: Energy output} = \text{HHV (biocrude)} \times \text{biocrude yield}$$

$$\text{Equation 8: Energy input} = Q_f + Q_w$$

$Q_f$  is the heat energy for heating 1 g of biomass

$Q_w$  is the heat energy for heating 7 g water

***Pigment quantification***

Pigments were extracted using a Soxhlet apparatus. Cloth filter bags containing

110 g of the centrifuged microalgal biomass was inserted in a soxhlet chamber fitted with a condenser and connected to a round bottom flask containing 100 mL of ethanol solvent (Kunene & Mahlambi, 2020). The solvent flask was refluxed for 24 hours at 85 °C (Kunene & Mahlambi, 2020). After the extraction, the sample was gone through the clean-up procedure by a centrifugation to remove any residual cell debris. Then, the pigments content was quantified using the Lichtenthaler and Wellburn modified method (LICHTENTHALER & WELLBURN, 1983).

### *Statistical Analysis*

The experiment was performed in duplicates. Results are represented as mean values, and standard error was used to represent error bars in the graphs.

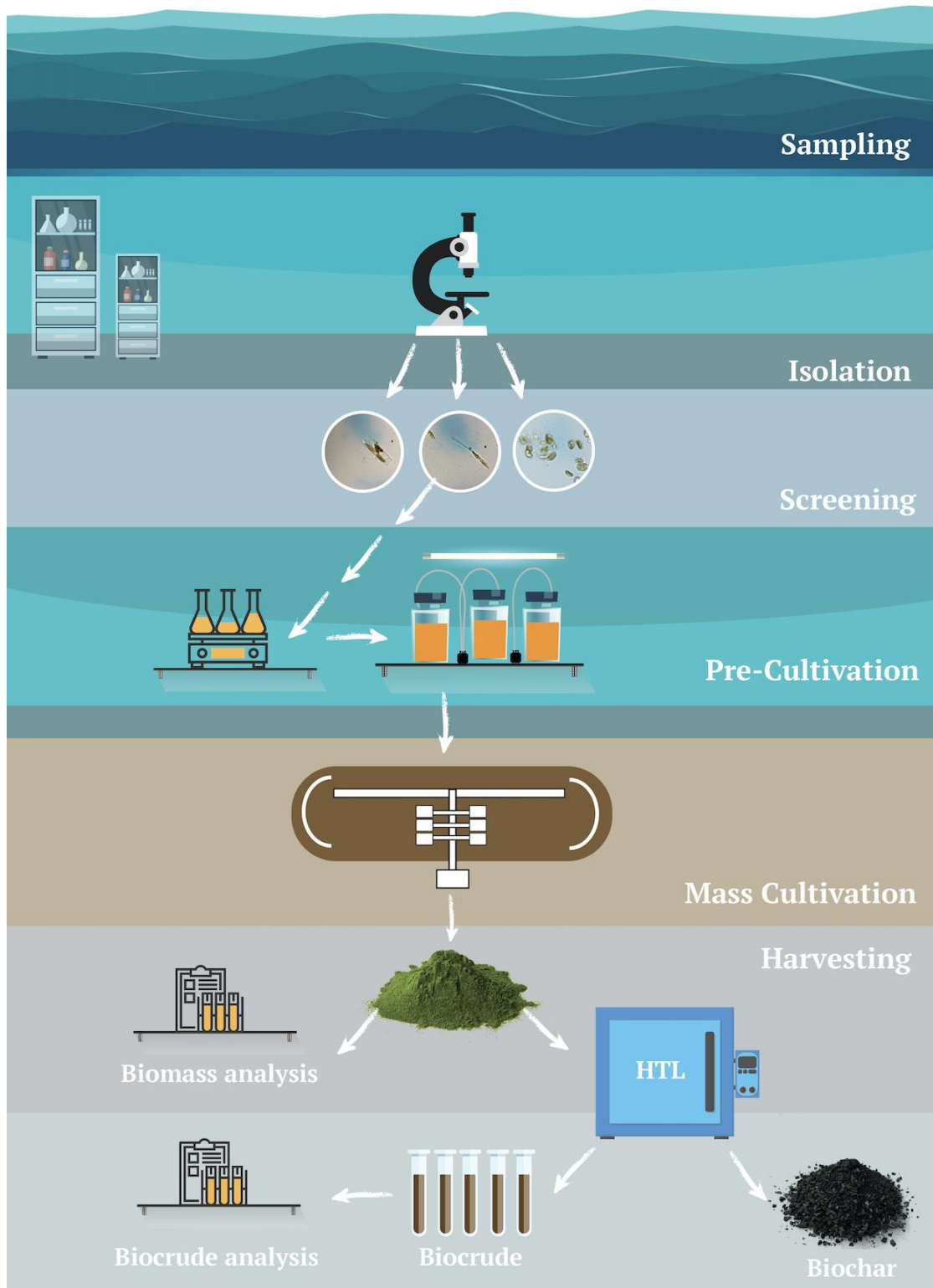




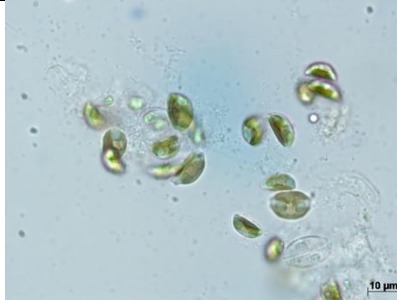
Figure 5: Methodology scheme diagram of this study

## CHAPTER 4: RESULTS AND DISCUSSION

### Screening of diatom strains

Among the three screened strains, *Trachyneis aspera* did not survive in the F/2 medium. *Nitzchia reversa* and *Amphora sp.* were selected for further screening. During the final screening, optimization of salinity levels, nitrogen source, and nitrogen concentration on *Nitzchia reversa*, and *Amphora sp.* growth were performed.

Table 6: Light microscopy image of a *Trachyneis aspera*, *Nitzchia reversa*, and *Amphora sp.* culture 100X magnification

Strain name	Light microscope image
<i>Trachyneis aspera</i>	
<i>Nitzchia reversa</i>	
<i>Amphora sp.</i>	

### ***Optimization of salinity levels on diatom growth***

In order to investigate the effect of salinity concentration on the growth of *Nitzchia reversa*, and *Amphora sp.* were cultivated in F/2 medium containing different salinity concentrations (40 ppt, 50 ppt, and 60 ppt). The growth curve of the selected diatoms exhibited different phases, starting with a lag phase, followed by a log phase, then a stationary phase, and ends with a death phase. The exponential growth reached the maximum after 8 days of cultivation for *Amphora sp.* under the three mentioned salinity concentration, where the exponential phase of *Nitzchia reversa* reached a maximum growth after 11 days of cultivation only under 40 and 60 ppt salinity concentrations (Figure 6). Figure 6 displays that the biomass growth of *Nitzchia reversa* decreased with increasing salinity as a general growth curve trend. The highest growth was at OD of 0.317 when *Nitzchia reversa* was grown at 40 ppt culture medium. Generally, both diatoms exhibited higher growth when they were grown at 40 ppt culture medium.



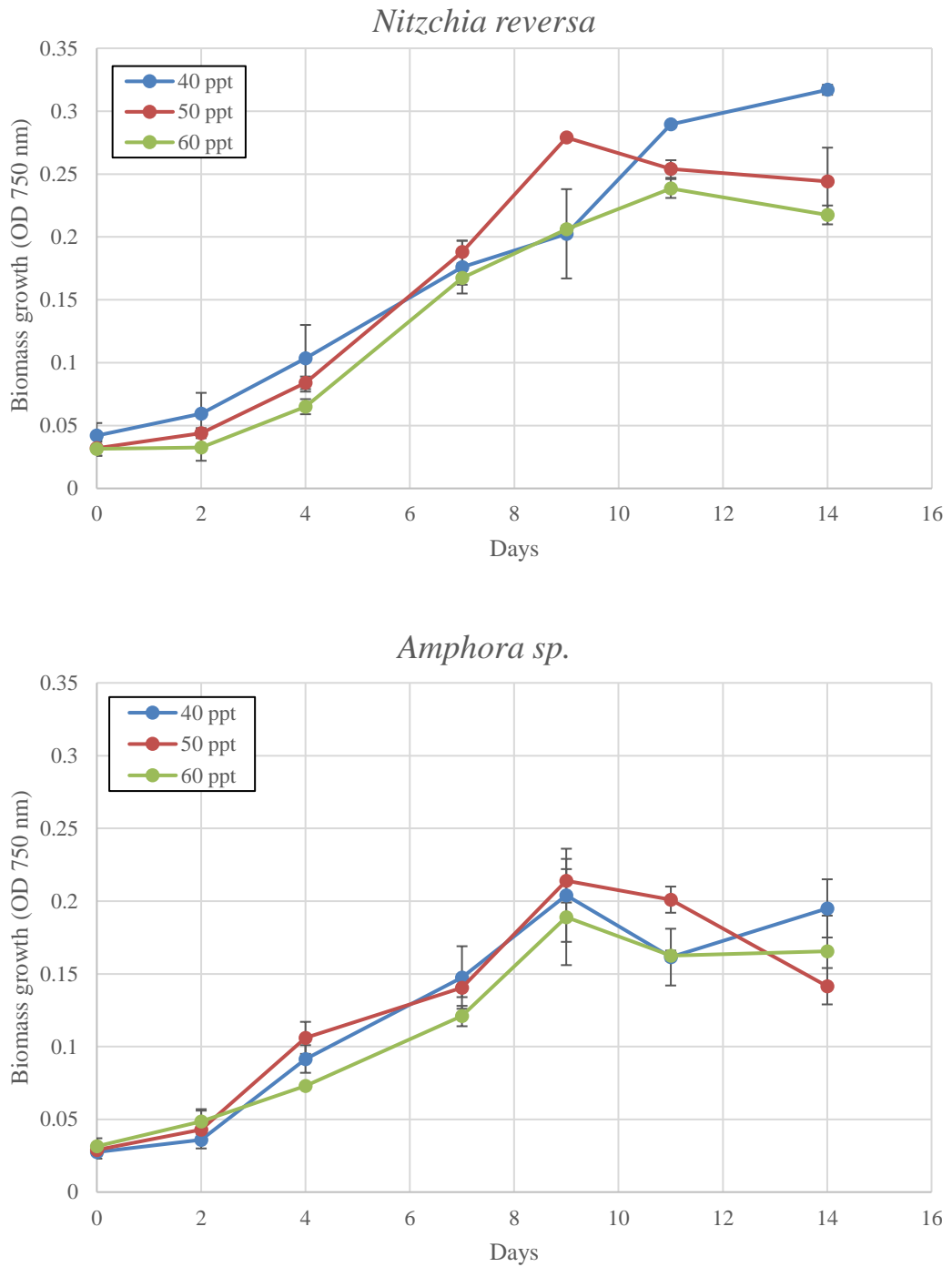


Figure 6: The growth of *Nitzchia reversa* (top) and *Amphora sp.* (bottom) under different salinity concentrations (error bar presents standard error where n =2)

### ***Optimization of nitrogen source on diatom growth***

Nitrogen is considered to be the major nutrient-limiting factor in the microalgal growth since it an essential requirement of proteins, nucleic acids, amino acids,

coenzymes, chlorophyll, and various photosynthetic pigments synthesis (Lin & Lin, 2011; Yodsuwan et al., 2017). According to various studies, it is very critical to identify the optimal nitrogen source and concentration of pure nitrogen to achieve the highest growth (Arumugam et al., 2013). Since the 40 ppt medium provided the optimum growth (Figure 8), a culture medium with 40 ppt was used to investigate the growth of *Nitzchia reversa* and *Amphora sp.* at different nitrogen sources. Figure 8 demonstrates the effects of the three nitrogen sources that have been investigated which are: sodium nitrate ( $\text{NaNO}_3$ ), ammonium chloride ( $\text{NH}_4\text{Cl}$ ), and urea ( $\text{CH}_4\text{N}_2\text{O}$ ). Among the different nitrogen sources that were tested, sodium nitrate and urea were found to be capable of supporting the growth of *Nitzchia reversa*. However, ammonium chloride was unable to support the growth of *Nitzchia reversa*. These findings were in accordance with an earlier report in the literature (Nayak et al., 2019). The highest biomass growth found when was cultivated with  $\text{NaNO}_3$  as the nitrogen source followed by cultivation in urea. A study reported that both sodium nitrate and urea resulted in a maximum sustainable yield of *Nannochloropsis salina* however, sodium nitrate exhibited a yield with larger cell size (Campos et al., 2014). Additionally, *Amphora sp.* showed a maximum biomass growth at OD of 0.3125 when subjected to sodium nitrate as a nitrogen source, which is significantly lower than what *Nitzchia reversa* achieved in the same conditions.

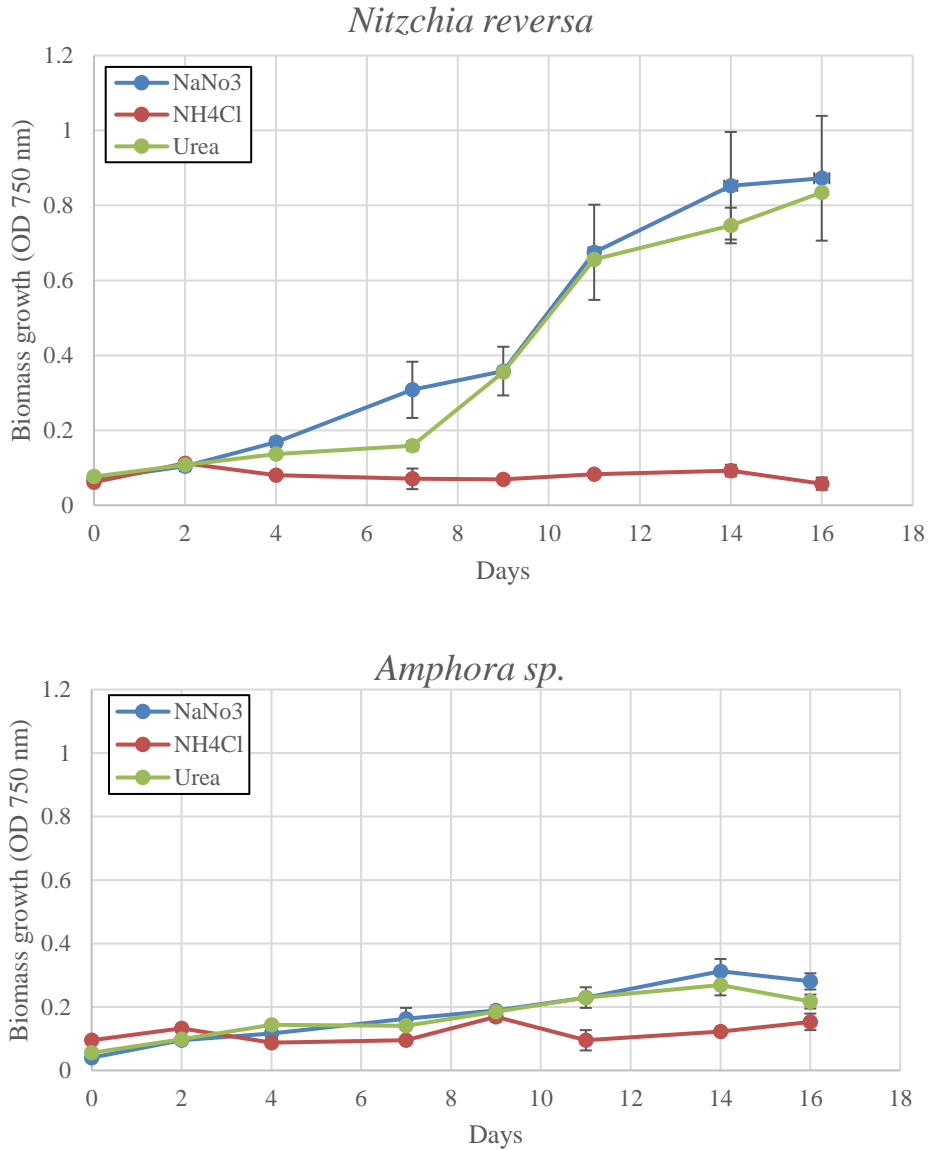


Figure 7: The growth of *Nitzchia reversa* (top) and *Amphora sp.* (bottom) under different nitrogen sources (error bar presents standard error where n =2)

### ***Optimization of nitrogen concentration on diatom growth***

As concluded in Figure 8, NaNO<sub>3</sub> was the favorable nitrogen source for both diatoms. *Nitzchia reversa* and *Amphora sp.* were further cultivated in 40 ppt F/2 medium with different concentrations of NaNO<sub>3</sub> as a nitrogen source. Figure 8 demonstrates comparisons of the effect of different NaNO<sub>3</sub> concentration (14, 28, and 42 mg NaNO<sub>3</sub>/L) on *Nitzchia reversa* and *Amphora sp.* It could be observed that the

biomass of *Nitzchia reversa* increased significantly faster when compared to *Amphora sp.* after the 4th day. Besides, the maximum biomass growth value for *Nitzchia reversa* was significantly higher than the maximum biomass growth value of *Amphora sp.*. Additionally, the highest biomass growth obtained was at OD of 0.9745 when *Nitzchia reversa* was cultivated with 42 mg NaNO<sub>3</sub>/L. In Figure 8, *Nitzchia reversa* exhibited a directly proportional relationship between nitrogen concentration and biomass growth. This trend was consistent with other findings that indicated that high nitrogen concentration leads to high algal biomass (Lin & Lin, 2011; Ördög et al., 2016; Yodsuwan et al., 2017). Through these screening investigations, *Nitzchia reversa* was selected as feedstock for biocrude production based on its growth potential which was measured using optical density in the screening process.

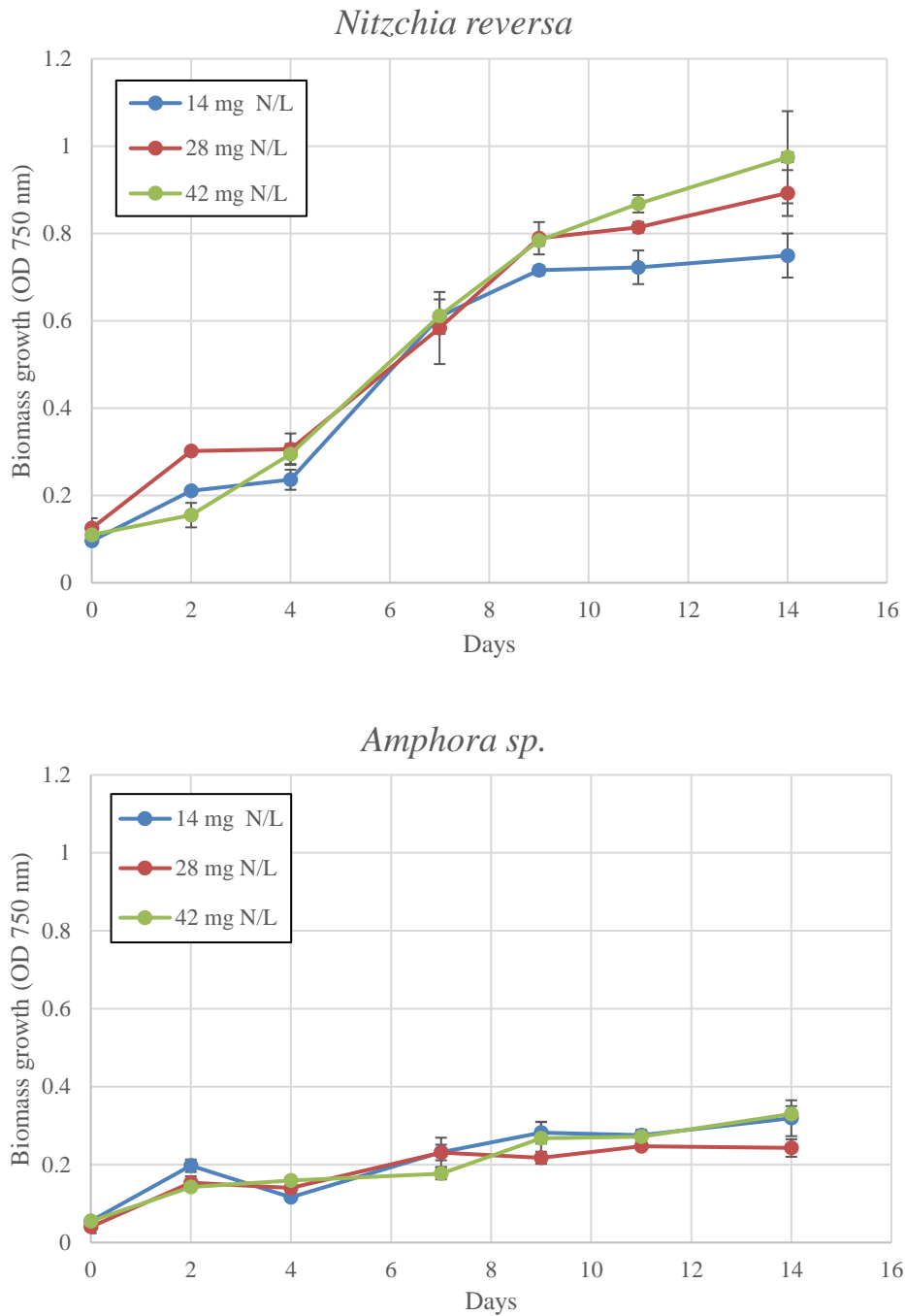


Figure 8: The growth of *Nitzchia reversa* (top) and *Amphora sp.* (bottom) under different sodium nitrate concentrations (error bar presents standard error where n =2)

### Characterization of *Nitzchia reversa* biomass

*Nitzchia reversa* was cultured in an outdoor raceway pond to obtain sufficient biomass in order to perform all the required analysis. Elemental characterization was

carried out through the measurement of the total carbon, hydrogen, nitrogen, and oxygen contents, followed by ash and HHV analysis using the obtained biomass. Table 7 lists the various characterizations of *Nitzchia reversas*’ biomass. The selected diatom strain had a high level of carbon compared to oxygen, nitrogen, and hydrogen levels, which is in agreement with most of the studies (Biller et al., 2012; Biller & Ross, 2011; Eboibi et al., 2014; B. Guo, Walter, et al., 2019; Palomino et al., 2020). The carbon content of different microalgal strains ranged between 42.0 % to 57.8 % (Eboibi et al., 2014; B. Guo, Walter, et al., 2019; Palomino et al., 2020). Compared to several microalgal strains, the carbon content of *Nitzchia reversa* (Table 7) falls amongst this range. *Nitzchia reversa* used in the reported study had a lower nitrogen content than *Chlorella vulgaris* (8.4 %), *Nannochloropsis gaditana* (7.4 %), *Nannochloropsis oculata* (8.6 %), *Tetraselmis sp.* (8 %), *Porphyridium cruentum* (8 %) and *Nannochloropsis oculata* (8.6 %) (Biller et al., 2012; Eboibi et al., 2014; B. Guo, Walter, et al., 2019). Besides, the ash content and the HHV of *Nitzchia reversa* biomass were 27.833% and 17.624 MJ/kg. Moreover, after the pigment extraction of *Nitzchia reversa*, the sample showed a high potential of fucoxanthin pigment Figure 9. However, further investigation should be performed regarding this matter. A corresponding recent study has reported an association between *Nitzschia laevis* and fucoxanthin (Sun et al., 2019).

Table 7: Elemental analysis, ash, and HHV of the *Nitzchia reversa* biomass

C (%)	H (%)	N (%)	O (%)	Ash (%)	HHV (MJ/kg)
43.028	7.478	6.922	42.572	27.833	17.624

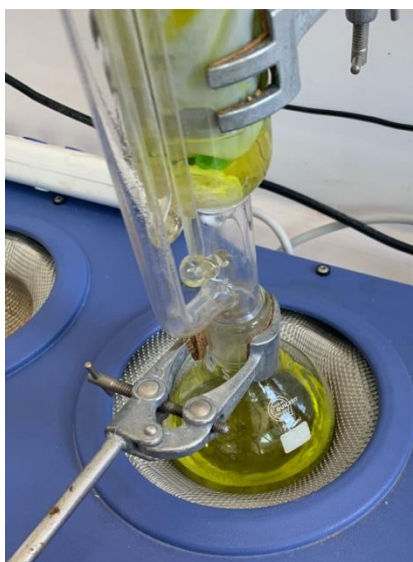


Figure 9: Pigment extraction

### **Biochemical composition of *Nitzschia reversa* biomass**

Generally, the biochemical composition of diatoms consists of lipids, carbohydrates, and proteins (Klin et al., 2020). Lipids serve as significant energy of diatoms (Klin et al., 2020; Sajjadi et al., 2018). Lipid's biological function is not limited to energy storage; they are also involved in the process of signaling (Maity et al., 2014). Carbohydrates also store energy in addition to carbon (Anthony W. D. Larkum et al., 2003; Sajjadi et al., 2018). Carbohydrates are critical intermediates in both photosynthetic carbon reduction and photorespiratory carbon oxidation cycles. In dark conditions, carbon dioxide is reduced to carbohydrates, and this process enables diatom to use the stored carbohydrates to survive in the dark (Anthony W. D. Larkum et al., 2003). Proteins perform essential functions in all the biological processes such as light-harvesting, cell growth, enzymatic reactions, and transport and storage (Conde et al., 2013; Klin et al., 2020).

Figure 10 illustrated the biochemical composition of the *Nitzschia reversa* analyzed in the present study. Carbohydrate was the main component of *Nitzschia reversa* biomass. The portion of the carbohydrate reached 47.7 % on a dry ash free

weight basis (DAF). A similar result was reported on the red microalgae *Porphyridium cruentum*, as 40 % (DAF) was carbohydrates (Biller & Ross, 2011). Compared to other diatoms, *Nitzschia reversa* has significantly higher carbohydrate content (Niccolai et al., 2019; Uriarte et al., 2006). The total carbohydrate content varied between 10.392 and 20.043 % (DAF) in most of the studied diatoms (Niccolai et al., 2019; Uriarte et al., 2006). The investigated *Nitzschia reversa* dry biomass exhibited lipid contents of 30.782 % (DAF), which is equivalent to 22.471 % (DW). *Nitzschia sp.* and *Nitzschia grossestriata*, which shared the same genus of the investigated strain has been reported to have a higher lipid content 30.5 % (DW) and 33.19 % (DW) (Y. C. Chen, 2012; Cointet et al., 2019). While *Nitzschia panduriformis* lipid content reached the maximum values of 39.88 % (DW), however, another study showed that *Nitzschia sp.* total lipid content varied from 12.5 to 30.51 % (DW) (Y. C. Chen, 2012; Cointet et al., 2019; Uriarte et al., 2006). Chen (2012) found that different diatom species such as *Melosira nummuloides*, *Navicula lyra*, *Amphora exigua*, and *Chaetoceros muelleri* exhibited high lipid contents of 32.84 %, 42.09 %, 44.95 % and 30.93 % (DW), respectively (Y. C. Chen, 2012). However, lower lipid content in different diatoms has been reported in the literature. Generally, *Navicula incerta*, *Biddulphia sp.*, and *Phaeodactylum tricornutum* consist of 28.177 %, 23.738 % and 24.061 % (DAF) lipid contents, respectively (Niccolai et al., 2019; Uriarte et al., 2006). The protein content detected in this study was 21.458 % DAF, which was similar to the value found in a previous study (Uriarte et al., 2006). For instance, Uriarte et al. (2006) obtained 20.866-24.191 % of protein content (DAF basis) in *Nitzschia sp.*. However, *Phaeodactylum tricornutum* exhibited a higher protein content that can reach as high as 45.54 % DAF (Uriarte et al., 2006) followed by *Biddulphia sp.*, which contains 27.830 % DAF protein (Niccolai et al., 2019).



Similarly, lower protein contents was reported in four diatom species (Uriarte et al., 2006). In particular *Nitzschia ovalis* and *Cylindrotheca closterium* which showed a protein content close to 5 % DW where *Cocconeis sp* and *Navicula incerta* showed a protein content close to 10 % DW.

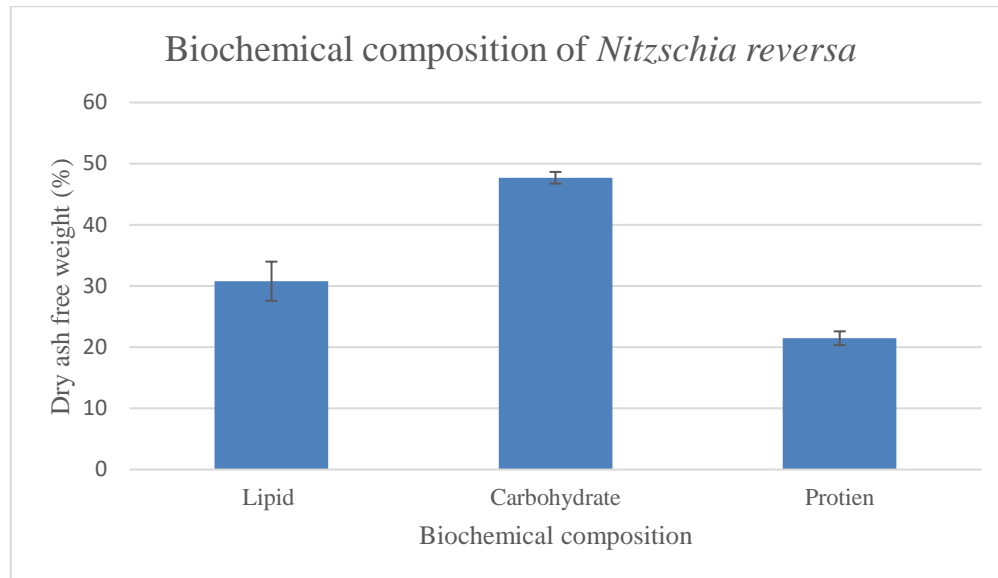


Figure 10: Distribution of elemental composition product and high heating value (HHV) obtained from hydrothermal liquefaction of *Nitzschia reversa* at different temperatures (error bar presents standard error where n =2)

### **Lipid content and fatty acid methyl esters (FAMES) of *Nitzchia reversa* biomass**

The investigated *Nitzchia reversa* in Table 8 showed fatty acids composition mainly constituted by Palmitic acid (C16:0) among saturated fatty acids. Oleic acid (C18:1) and Gadeloic acid (C20:1) among monounsaturated fatty acids, EPA (C20:5), and DHA (C22:6) among polyunsaturated ones. Fatty acids has been widely associated with a positive influence on human health. For example, studies have determined that both DHA and EPA have various health benefits (Arab-Tehrany et al., 2012). The contents of DHA (13.046%) found in *Nitzchia reversa* in the present

study were significantly higher compared to eight diatom species (0.37 %-1.29 %) studied by Chen, (2012). *Nitzchia reversa* also exhibited a high EPA content that reached to 10.88 %. According to the published studies, the EPA of different diatom species could be as high as 30.85 % (Y. C. Chen, 2012; Duong et al., 2015; Niccolai et al., 2019). The studied *Nitzchia reversa* EPA value (10.88 %) is within this range. However, *Nitzchia reversa* exhibited higher EPA content (Table 8) than *Nitzschia panduriformis* (8.61 %) and *Nitzschia grossestriata* (3.37 %), which shared the same genus (Y. C. Chen, 2012). Both DHA and EPA have the ability to reduce heart disease risk, reduce the blood pressure and support the blood circulation (Allaire et al., 2016; X. Guo et al., 2019; Sekikawa et al., 2019). More importantly, DHA and EPA have been linked to a decreased chance of depression and Alzheimer's disease (Che et al., 2018; Heras-Sandoval et al., 2016; Patrick & Ames, 2015; Yassine et al., 2017). Besides, DHA and EPA help to counteract symptoms in rheumatoid arthritis and muscle soreness due to their anti-inflammatory properties. (Dasilva et al., 2015; Dawczynski et al., 2018; Tsuchiya et al., 2016; Wall et al., 2010). There are substantial evidence that DHA supplements improved the behavior or attention in attention deficit hyperactivity disorder (ADHD) patients (Bonvicini et al., 2016; J.-R. Chen et al., 2004). In addition, DHA exerts a positive influence on reducing the risk of cancer progression because of its anti-inflammatory characteristics (Ortea et al., 2018; Yum et al., 2016).

As shown in Table 8, palmitic acid was the primary fatty acids comprising 17.397 % of the total fatty acid, followed by Oleic acid (14.064 %). Comparable results were obtained for *Nitzschia grossestriata* as palmitic acid (15.07 %), and Oleic acid (18.86 %) were the major fraction of its total fatty acid (Y. C. Chen, 2012). Studies have shown that oleic acid displays an essential role in fighting type 2 diabetes

mellitus and cardiovascular diseases (Granado-Casas & Mauricio, 2019). Besides, palmitic acid has been used in the cosmetics sector (Hubbard, 2007). Gadeloic acid content in most of the reported diatoms varied between 0.19 to 3.55 %, which is far lower than gadeloic acid content (9.797% ) in the presented study (Y. C. Chen, 2012). Compared to the presented study, Chen, (2012) found higher contents of myristic acid and plamitoleic acid that reached to 77.41 % and 19.21 % of total fatty acid. The rest of the fatty acids, such as myristoleic acid, linoleum acid, linolenic acid, arachidic acid, eicosadienoic acid, elaeostearic acid, behenic acid, erucic acid, lignoceric acid, and nervonic were relatively low concentration. These results appear consistent with fatty acid profiles reported for different diatoms (Y. C. Chen, 2012; Niccolai et al., 2019). Hubbard, (2007) reported that gadeloic acid, myristic acid, and palmitic acid are critical components in the cosmetics industry where palmitoleic acid is known for its pharmaceutical applications (Parveez et al., 2012).

Table 8: Fatty acid composition and profile of *Nitzchia reversa*

Common name of fatty acid	Formula	Percentage %
Myristic acid	C14:0	6.510
Myristoleic acid	C14:1	1.110
<b>Palmitic acid</b>	<b>C16:0</b>	<b>17.397</b>
Plamitoleic acid	C16:1	5.435
<b>Oleic acid</b>	<b>C18:1</b>	<b>14.064</b>
Vaccenic acid	C18:1	4.336
Linoleum acid	C18:2	2.202
Linolenic acid	C18:3	2.166
Arachidic acid	C20:0	1.066

Gadeloic acid	C20:1	9.797
Eicosadienoic acid	C20:2	1.094
Arachidonic acid	C20:4	3.207
Elaeostearic acid	C20:3	1.084
<b>EPA</b>	<b>C20:5</b>	<b>10.880</b>
Behenic acid	C22:0	1.092
Erucic acid	C22:1	3.265
Lignoceric acid	C24:0	1.122
<b>DHA</b>	<b>C22:6</b>	<b>13.046</b>
Nervonic acid	C24:1	1.126

### **Effect of hydrothermal liquefaction operating temperature on the products**

#### ***Operating temperature***

Figure 12 demonstrates the effect of temperature on the product yields after HTL of *Nitzschia reversa* from 300 to 400 °C for a fixed duration of 30 minutes. HTL treatment at the lowest temperature (300 °C) resulted in the lowest biocrude yield (36.557 %). With an increase in the temperature, the biocrude yield increased until the temperature reached 375 °C; after 375 °C, the biocrude yield declined. Studies reported that under low temperatures, the low yield was attributed to predominant role of hydrolysis of the biomass, the dissolving of organic matter in the aqueous layer, and the limited conversion to biocrude and gas (Eboibi et al., 2014; Han et al., 2019). In the other hand, the decline of biocrude yield at 400 °C might be due to the production of gaseous products at high temperatures (Eboibi et al., 2014). Generally, the obtained results revealed that *Nitzschia reversa* biocrude yield had an upward tendency with the increase of the temperature. Similar trends of HTL biocrude versus temperature were

observed, and this trend could be attributed to the fact that high temperatures can promote the reactions of hydrolysis, transformation, and repolymerization in the HTL process (Eboibi et al., 2014; He et al., 2020; Yulin Hu et al., 2019). HTL treatment at intermediate temperatures (350 °C and 375 °C) led to the highest biocrude yield (52.189 % and 57.273 %). It is expected that the high biocrude content is attributed to the high lipid content of *Nitzschia reversa* biomass (30.782 % DAF) (P. Das et al., 2019). Generally, the biocrude content in this study was higher than those reported in other investigations (Biller et al., 2012; Biller & Ross, 2011; P. Das et al., 2019; Vardon et al., 2011). *Nitzschia reversa* showed a highest biocrude yield of 57.2 % (DAF) obtained at 375 °C and having an HHV of 27.434 MJ/kg. These results are consistent with a study reported that the maximum biocrude yield (49.4 %) of *Desmodesmus sp.* was also produced from 375 °C HTL reaction. Still, with much less reaction time (5 min) and higher HHV (35.4 MJ/kg), this result supports the possibility of optimizing the HTL by low reaction time (Garcia Alba et al., 2012). Another study showed that *Tetraselmis sp.* exhibited comparable biocrude content (50.8 % DAF) obtained from HTL processed at 350 °C with lower HHV (21.82 MJ/kg) (P. Das et al., 2019). However, At 350 °C HTL treatment temperature, *Nitzschia reversa* produced higher biocrude content (52.189 % DAF). Compared to the studied biocrude content from *Nitzschia reversa* (Figure 12) *Chlorella vulgaris*, *Nannochloropsis occulta*, *Porphyridium*, *Chlorella*, and *Scenedemus* produced lower biocrude yield ranged approximately from 21.5 % DAF to 35.8 % DAF, and lower HHV ranged from 33.6 MJ/kg to 35.1 MJ/kg obtained at 350 °C of 1-hour HTL treatment (Biller et al., 2012; Biller & Ross, 2011). At HTL 325 °C reaction temperature, Das et al. (2019) reported that *Chlorocystis sp.* and *Picochlorum sp.* exhibits biocrude content of 34.8 % DAF and 39.6 % DAF which is less than what was achieved in this study (40.8 % DAF) at the same HTL reaction

conditions (P. Das et al., 2019). However, at 300 °C reaction temperature and 1 hour reaction time of HTL, Biller et. (2012) reported higher biocrude content of *Chlorogloeopsis sp.* (38.6 % DAF) and *Chlorella sp.* (46.6 % DAF) biomass and than what obtained from this study (36 % DAF).

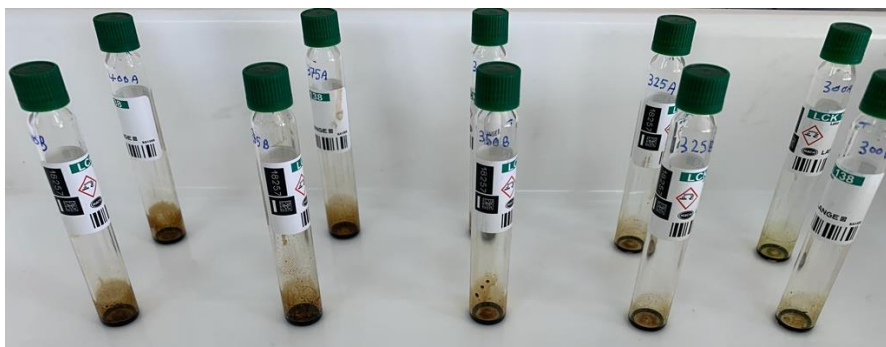


Figure 11: Biocrude samples obtained from hydrothermal liquefaction of *Nitzschia reversa* at different temperatures

The effect of HTL temperature on biochar is shown in Figure 12, where the highest biochar content was found at 325 °C, and it continued to decline to a minimum value at 375 °C. The domination of hydrothermal liquefaction and gasification reactions operating at extreme temperatures could be the reason behind the reduction of biochar content (Probir Das et al., 2020). *Nitzschia reversa* showed an inverse relationship between the biochar and the biocrude content. Basically, as the biocrude content increased, the biochar content decreased at the intermediate temperature (325 °C - 375 °C). The trend of microalgal biocrude verses biochar is in agreement with those obtained in similar studies (Garcia Alba et al., 2012; He et al., 2020; Palomino et al., 2020). 22.682% (DAF) was the content of biochar obtained at 325 °C HTL treatment, which is higher than what Das et al. (2019) presented (18.0 % DAF for *Chlorocystis sp* and 12.15% DAF for *Picochlorum sp.*) at the same HTL treatment

condition (P. Das et al., 2019). For the HTL reaction conducted at 350 °C, *Nitzschia reversa* shows biochar content of 15.741 %. A biochar yield of 15 % was reported for *Tetraselmis sp.* biomass at 350 °C (Probir Das et al., 2019). Nevertheless, the obtained biochar could be used as a soil fertilizer, animal feed additive, and a removing agent of organic pollutants from wastewater (Yulin Hu et al., 2019).

At higher temperature of HTL, hydrothermal gasification (HTG) reactions led to an increase of gaseous compounds (Probir Das et al., 2020). From 325 °C to 400 °C, the gas and loss contents of *Nitzschia reversa* presented a general increasing trend (from 36.491 % to 52.882 %) despite the decline at 350 °C (32.16%). This trend is in good accord with a study which reported that the increase of HTL reaction temperature (260 °C to 340 °C) led to the increase of the gas content mainly for *Nannochloropsis sp. biomass* (15.95 % to 36.97 %), despite the decline at 320°C (20.83 %) (He et al., 2020). Compared to different studies, a high gas product was exhibited from *Nitzschia reversa*, possibly a result of a high carbohydrate content of *Nitzschia reversa* biomass, since it is reported that carbohydrates are more accessible to decompose to gas products by HTL (B. Guo, Yang, et al., 2019).

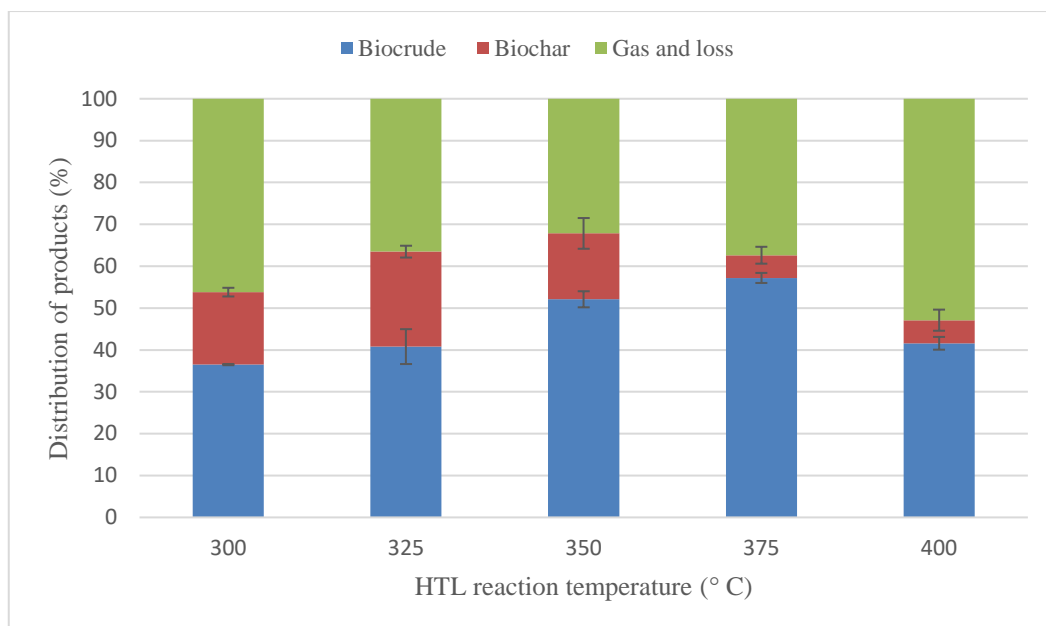


Figure 12: Distribution of various product obtained from hydrothermal liquefaction of *Nitzschia reversa* at different temperatures (error bar presents standard error where n =2)

### ***Higher heating values of the biocrude***

The elemental composition (C, H, N, and O) of the biocrude samples and their corresponding higher heating values (HHV) were presented in Figure 13. Generally, the biocrude produced from *Nitzschia reversa* had a high carbon content. It is more desirable for the biocrude obtained from hydrothermal liquefaction to have high carbon content as it would increase the higher heating value (HHV) of the biocrude (Biller & Ross, 2011, 2016). In contrast to this study, the highest carbon content (69.825 %) obtained from the lowest HTL temperature reaction (300 °C) was corresponding to the highest HHV (35.114 MJ/kg). According to previously published studies of different microalgal strains operated at different HTL reaction conditions, the carbon content ranged from 61.12 % to 85.43 % (Biller et al., 2012; Biller & Ross, 2011; P. Das et al., 2019; Eboibi et al., 2014; B. Guo, Walter, et al., 2019; Li & Savage,



2013; Palomino et al., 2020; Ren et al., 2018). The carbon content obtained of *Nitzschia reversa* biocrude falls within this range. Studies have reported a close carbon content of the microalgal biocrude obtained from a comparable HTL temperature (300°C -310 °C), and higher HTL reaction time (60 min) (Biller et al., 2012). However, with the same operating temperature and lower HTL reaction time (10-15 min ), studies reported that *Botryococcus braunii* and *Chlorella vulgaris* exhibit biocrude with lower carbon content (61.12% and 68.8%) (Palomino et al., 2020; Ren et al., 2018). Li & Savage (2013) showed that at 400 °C HTL, *Nannochloropsis sp.* produced biocrude with significantly high carbon content (85.43%), however with same temperature, *Nitzschia reversa* in this work yielded lower carbon content (60.252%) (Li & Savage, 2013). As showed in Figure 13, the highest carbon content (69.825 %) obtained from the lowest HTL temperature reaction (300 °C) was corresponding to the highest HHV (35.114 MJ/kg). At 300 °C HTL reaction, *Tetraselmis sp.*, *Nannochloropsis sp.*, and *Sargassum sp.* exhibited a carbon content of 67%, 74.82%, and 73.56% with HHV of 31.1 MJ/kg, 35.92MJ/kg, and 33.63MJ/kg, respectively (Han et al., 2019; He et al., 2020). Furthermore, He et al. (2020) reported that both *Nannochloropsis sp.*, and *Sargassum sp.* at different HTL temperature (from 260 to 340 °C) produced biocrude with minimum carbon content (72.15% and 71.74%) and HHV value ( 35.92 and 33.63 MJ/kg ) at 260 °C. Where maximum carbon content (75.70% and 74.99) and HHV value (37.88 and 35.23 MJ/kg) obtained at 260 C.

During HTL reactions, oxygen is recovered mainly as H<sub>2</sub>O and through a range of dehydration and decarboxylation reactions, eventually leading to an increase in carbon content in the biocrude plus improve the biocrudes' H/C atomic ratio (Eboibi

et al., 2014). Studies have revealed that a reduction of oxygen content leads the biocrude to be more stable during storage, besides improving other properties, such as HHV and viscosity (Palomino et al., 2020). It's been published that biocrude associated with a low oxygen concentration enhances the HHV (Biller & Ross, 2011; Ren et al., 2018). The results of this research support what has been published, as that the lowest oxygen content of the biocrude (17.578 %) led to the highest HHV (35.144 MJ/kg). Comparable results were reported, *Tetraselmis sp.* exhibited 14% of oxygen from biocrude produced at 310 °C HTL reaction with HHV of 35.0 MJ/kg (Eboibi et al., 2014). As presented in Figure 13, in higher temperature (350 °C), the oxygen content increased to reach 27.591 %, and HHV decreased to reach 24.734 MJ/kg. Ren et al, (2018) reported similar trends of low HHV (30 MJ/kg) and high oxygen content (27.21 %) biocrude produced from *Batryococcus braunii*. The oxygen content and HHV of the biocrude have an inverse relationship. Besides, the high oxygen content can be due to the fact that *Nitzschia reversa* biomass consisted of high carbohydrate content, for instance, Biller & ross (2011) found that high carbohydrate content corresponds to high oxygen content (Biller & Ross, 2011). As shown in Figure 13, the reaction temperatures of 350 and 400 °C resulted in higher oxygen content which could be due to the fact that high temperatures were in favor of the generation high oxygen content. The high oxygen might be coming from the formation of ketones, esters, phenols and other oxygen functional groups. Oxygenates contribute to the relatively high oxygen of content in HTL biocrude oil. At higher temperature, formation of oxygen-containing compounds is observed. According to the literature conversion of organic acids to alcohols via reduction could occur at higher temperatures (Hu et al., 2019). Beside He et al. (2020) reported that Ketones mainly include cyclopentenones and cyclohexanones originating from Retro-Aldol

condensation and further cyclization of monosaccharide, whose content increased with increasing temperature. Higher temperature is in favor of the cyclization reaction of small molecules and hence increases the production of ketones (He et al., 2020).

HTL microalgae biocrude reported to have high nitrogen content because nitrogen is an essential nutrient for microalgae growth (Obeid et al., 2020). The existence of elevated nitrogen fraction in the biocrude oil is poses difficulties and challenges for the petroleum refining industry. Since the presence of nitrogen in the fuel contributes to NO<sub>x</sub> emission, high concentration of nitrogen in the oil is unfavorable for environmental and legislative reasons (Biller & Ross, 2011). Similarly, Obeid et al. (2020) proved that biocrude with high nitrogen content causes high NO<sub>x</sub> emission. As presented in Figure 13, higher nitrogen content produced at higher temperatures led to low HHV, and this trend was similar to most studies on microalgal HTL (Biller et al., 2012; Biller & Ross, 2011; P. Das et al., 2019; Probir Das et al., 2020). Biocrude is differentiated from other petroleum crudes by the crucial factor of high nitrogen (Vardon et al., 2011). According to different studies, the nitrogen content of HTL microalgal biocrude ranged between 1.92 % to 15.1 % (Biller et al., 2012; Biller & Ross, 2011; P. Das et al., 2019; Eboibi et al., 2014; B. Guo, Walter, et al., 2019; Li & Savage, 2013; Palomino et al., 2020; Ren et al., 2018). Compared to this range, the investigated biocrude exhibited a low nitrogen content as it gave the minimum nitrogen content (2 %) and maximum HHV (35 MJ/kg) from HTL operated at 300 °C. The fact behind the low percentage (2.318 %) is that nitrogen is essentially originated from the protein portion, and the protein content was the lowest in *Nitzschia reversa* biomass (Biller et al., 2012; Biller & Ross, 2011; Eboibi et al., 2014). Even though the obtained biocrude had 2.318 % nitrogen, it is still

considered undesirably high (Biller & Ross, 2011). However, a recent study investigated the influence of nitrogen content in fuels of an industrial multi-cylinder diesel engine. They succeeded to prove that emissions from fuel contained 0.1 % nitrogen, 0.5 % nitrogen, and 2 % nitrogen, which were lower than EUROII standard (4 g/kWh) (Obeid et al., 2020). These findings corresponds to the results obtained from 300°C HTL biocrude.

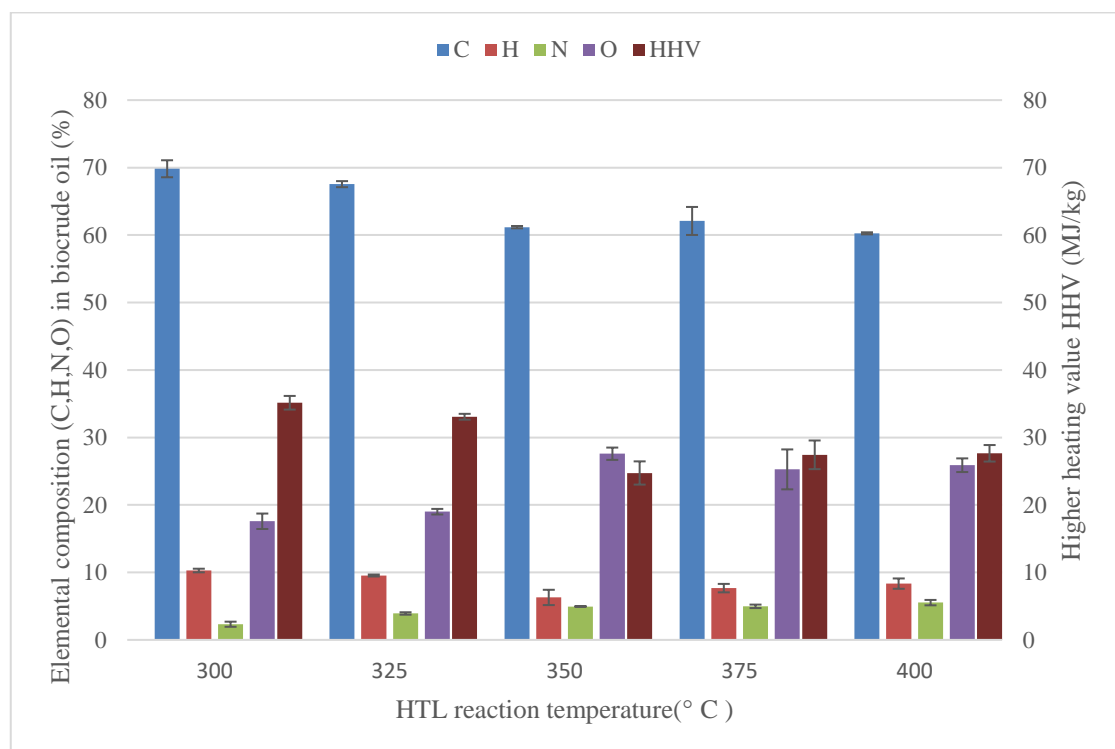


Figure 13: Distribution of elemental composition (C, H, N, and O) product and high heating value (HHV) in biocrude samples obtained from hydrothermal liquefaction of *Nitzschia reversa* at different temperatures (error bar presents standard error where n =2)

## Distribution of hydrocarbons in the biocrude obtained from hydrothermal liquefaction

The biocrude organic compounds were classified into three major groups: alkanes, alkenes, and polyaromatic, and other hydrocarbons (Figure 14). In general, alkene, alkane, and their derivatives are aliphatic, while the aromatic compounds consist of benzene, phenol, p-cresol, styrene, naphthalene, and their derivatives (Hable et al., 2019). As shown in Figure 14, polyaromatic and other hydrocarbons were significantly abundant in all biocrude samples, these results are in good agreement with earlier published biocrude studies (Probir Das et al., 2020; Mishra & Mohanty, 2020). In all biocrude samples, the alkane compounds were higher than the alkene compounds except for the sample that has been processed at 325 °C HTL. Das et al. (2019) obtained biocrude from *Chlorocystis sp.* and reported that its' alkane content was composed mainly of the following: nonane, octane, heptane, hexadecane, cyclohexane, and cyclopentane. Similar results were obtained in this present study but with different GC/MS peak areas. Figure 14 shows that when HTL temperature increased from 300 to 350 °C, alkanes compounds slightly decreased from 10.909 % to 9.589%. After reaching 350 °C, alkanes compounds increased to reach 13.174 %. On the other hand, alkene compounds decreased during the temperature increase between 325 °C to 400 °C from 10 % to 2.994 %. Furthermore, the major compound that demonstrated the highest peak at 325 °C HTL was an alkene (bicyclo[4.2.0]oct-7-ene). Based on the peak areas of GC/MS biocrude analysis, the major peak areas were fatty acid ester compounds. In particular, the dominant peak areas at 300, 325, 350, and 375 °C HTL biocrude were octadecanoic acid (10.4 %), hexadecanoic acid (76.78 %), tetradecanoic acid (35.43 %), and hexadecanoic acid (8.39 %). The fatty acids esters are formed mainly from the hydrolysis of biomass lipids (Mishra &

Mohanty, 2020; Parsa et al., 2018). A study reported that biofuel with high esters content could improve ignition qualities (Mishra & Mohanty, 2020).

However, at 400 °C HTL the highest peak area was 1.48 %, and the corresponding compound was pyrrolidine which was characterized by nitrogenates compound. It has been stated that at high HTL temperatures, the hydrothermal gasification process becomes the dominant process, which causes the reduction of total carbon content and the increase of gaseous compounds (Probir Das et al., 2020). Where the obtained nitrogenates compounds could be formed through dehydration of proteins and amides of the biomass (Mishra & Mohanty, 2020). Hu et al. (2019) reported that the major nitrogenates compounds present in the microalgal biocrude were indole, pyrrole, pyrrolidine, pyridine, pyrimidine, imidazole, nitrile, and pyrazine. The nitrogenous compounds, in the biocrude samples- obtained in this study, were consistent with the previous studies, due to the fact that all these nitrogenate compounds were present in high HTL temperature, mainly at 400 °C HTL. According to Hu et al. (2019), the major amides compounds in the biocrude obtained from HTL of microalgae were tetradecanamide and decanamide. Compared to this study tetradecanamide and decanamide compounds were found in biocrude samples that were produced under intermediate HTL temperatures (325, 350 and 375 °C). Furthermore, a study stated that aldehyde, ketone, carboxylic acid, and alcohol were the common oxygenate compounds in different biocrude samples produced from various microalgae by HTL (Yulin Hu et al., 2019). The oxygenate compounds of microalgal biocrude are in line with this present study. Aldehyde compounds were observed at 300, 350, and 400 °C HTL biocrude, while ketone compounds observed at 300 and 400 °C HTL biocrude. Carboxylic acid area peaks were mainly observed at 400 °C HTL biocrude, where alcohol compounds were observed only at 400 °C

HTL biocrude.

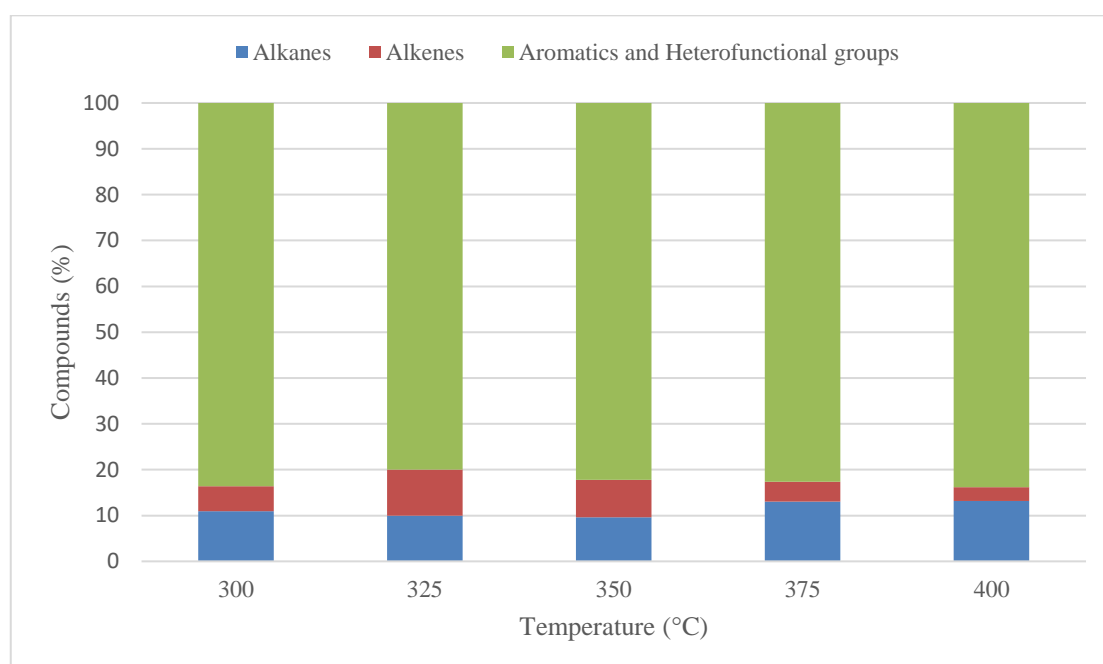


Figure 14: Distribution of organic compounds in biocrude samples obtained from hydrothermal liquefaction of *Nitzschia reversa* at different temperatures

### Energy recovery potential

Energy return on investment (EROI) is to measure the energy returned to the economy and society compared to the energy required to obtain that energy (Yan Hu et al., 2013). Where energy recovery (ER) is to measure the energy content in HTL oil to the energy content of the feedstock (Zhang & Chen, 2018). The EROI and ER of the biocrude processed at different HTL temperatures are shown in Figure 15. Studies have reported that the EROI value should be greater than 1 in order to be considered profitable, and the higher the EROI value, the higher the viability (Bauer et al., 2018). Figure 15 indicates that all EROI values met the required conditions as all of them were greater than 1. These EROI values correspond to various EROI values of HTL biocrude produced from different microalgal strains (Bauer et al., 2018).

Generally, It has shown that EROI and ER have a direct relationship; this can be attributed to the fact that biocrude yield and HHV have a significant influence on ER and EROI (Probir Das et al., 2020; Mishra & Mohanty, 2020). The maximum values of EROI (1.682) and ER (64.271% ) were produced at a similar HTL temperature (375 °C ) of the maximum biocrude yield. Furthermore, Biocrude obtained from *Nannochloropsis sp.* biomass showed a higher ER content (73 %) when it was processed at a 375 °C HTL temperature. (Garcia Alba et al., 2012). At 400 °C, both EROI and ER declined to minimum values reaching 1.235 and 47.209 %. Similar trends were reported by Garcia et al. (2012). Besides, das et a. (2020) reported that the formation of more gaseous products at high HTL temperature was correlated to the reduction of EROI and ER. However, in the presented study, the ER of biocrude produced at low HTL temperatures ( 300 and 325 °C) exhibited a lower ER content compared to earlier studies (Garcia Alba et al., 2012; Han et al., 2019; He et al., 2020). Biocrude of 75.99 % and 71% ER was obtained from *Nannochloropsis sp.*, and *Desmodesmus sp.* respectively, when processed at 300 °C HTL (Garcia Alba et al., 2012; He et al., 2020). Nevertheless, Han et al. (2019) reported a close biocrude ER content (55.5 %) of *Nannochloropsis sp.* produced from 300 °C HTL. At HTL 325 °C reaction temperature, studies reported that *Tetraselmis* and *Desmodesmus sp* exhibited an ER of 60 %, which is more than what was achieved in this study at the same HTL temperature (Garcia Alba et al., 2012; Han et al., 2019). According to different studies, the ER content of 350 °C HTL microalgal biocrude ranged between 51.6% to 83.2%. The investigated ER biocrude obtained from 350 °C HTL showed a comparable content (Biller & Ross, 2011; Garcia Alba et al., 2012; Gu et al., 2020; Han et al., 2019).



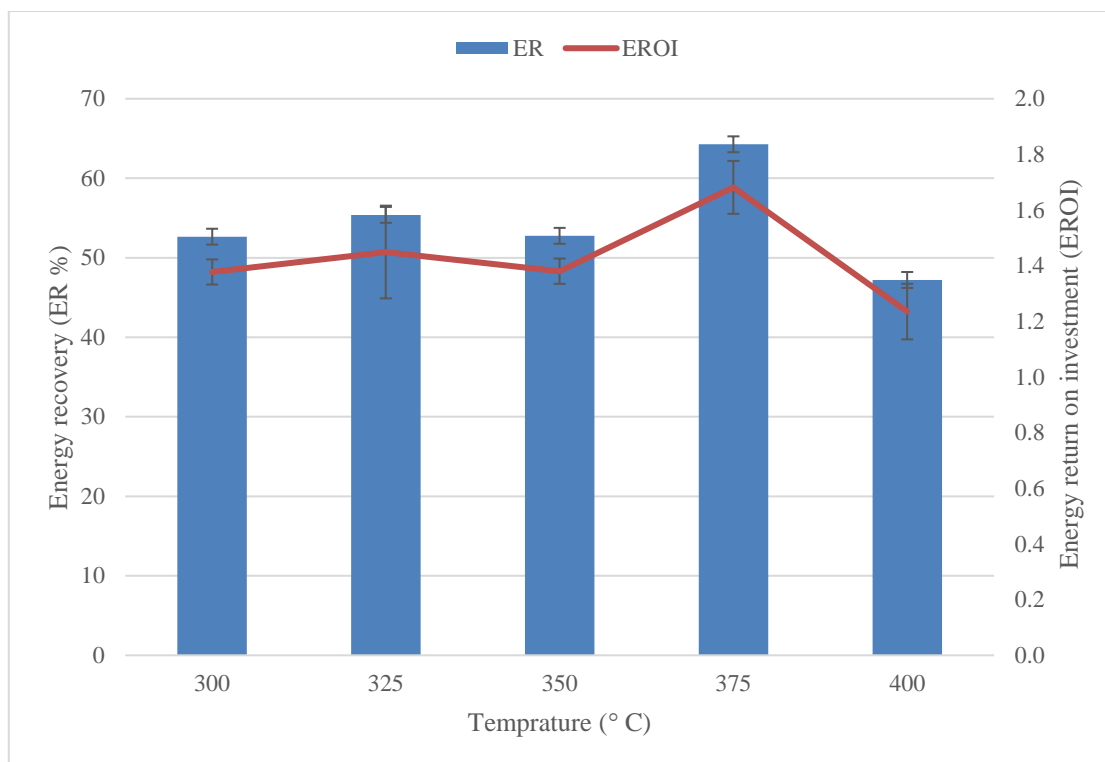


Figure 15: Energy recovery on investment (EROI) and energy recovery (ER) values of biocrude production from *Nitzschia reversa* by hydrothermal liquefaction at different temperature ( error bar represents standard error, where n =2 )

## CHAPTER 5: CONCLUSION

The potential of obtaining an efficient biocrude product from the primary biomass has been demonstrated repeatedly in the literature. However, this study explored a suitable diatom species that has not been investigated in previous studies, which resulted in biocrude characteristics that are highly desirable. This is also considered to be a pioneer study in optimizing the growth of the selected diatom on a large scale under natural conditions and convert the biomass into biocrude oil using the HTL technique. Although the study has its strengths, there were some limitations -faced during the process including the death of diatoms during the first phase of the study, the inability to examine the sulfur content in the biocrude, in addition to the restricted ability of our HTL process to identify and quantify the gaseous byproducts. Also, the emission of NO<sub>x</sub> from the biocrude is highly undesirable; hydro-treatment of biocrude is one possible method to overcome these emissions, which should be done in future research. Lastly, the existing pigments in diatoms, including fucoxanthin, could be extracted before the conversion of the biomass to biocrude; these pigments have high value and could be utilized in the pharmaceutical sector. The biorefinery options of the produced biomass could make the overall process of biocrude production more economical. However, these aspects need to be explored in future studies.

## REFERENCES

- Allaire, J., Couture, P., Leclerc, M., Charest, A., Marin, J., Lépine, M. C., Talbot, D., Tchernof, A., & Lamarche, B. (2016). A randomized, crossover, head-to-head comparison of eicosapentaenoic acid and docosahexaenoic acid supplementation to reduce inflammation markers in men and women: The Comparing EPA to DHA (ComparED) Study. *American Journal of Clinical Nutrition*, *104*(2), 280–287. <https://doi.org/10.3945/ajcn.116.131896>
- Anthony W. D. Larkum, Douglas, S. E., & Raven, J. A. (2003). *Photosynthesis in Algae*. Springer. <https://doi.org/10.1007/978-94-007-1038-2>
- Arab-Tehrany, E., Jacquot, M., Gaiani, C., Imran, M., Desobry, S., & Linder, M. (2012). Beneficial effects and oxidative stability of omega-3 long-chain polyunsaturated fatty acids. *Trends in Food Science & Technology*, *25*(1), 24–33. <https://doi.org/https://doi.org/10.1016/j.tifs.2011.12.002>
- Arumugam, M., Agarwal, A., Arya, M. C., & Ahmed, Z. (2013). Influence of nitrogen sources on biomass productivity of microalgae *Scenedesmus bijugatus*. *Bioresource Technology*, *131*, 246–249. <https://doi.org/10.1016/j.biortech.2012.12.159>
- Athanasakoglou, A., & Kampranis, S. C. (2019). Diatom isoprenoids: Advances and biotechnological potential. *Biotechnology Advances*, *37*(8), 107417. <https://doi.org/10.1016/j.biotechadv.2019.107417>
- Bauer, S. K., Reynolds, C. F., Peng, S., & Colosi, L. M. (2018). Evaluating the Water Quality Impacts of Hydrothermal Liquefaction Assessment of Carbon, Nitrogen, and Energy Recovery. *Bioresource Technology Reports*. <https://doi.org/10.1016/j.biteb.2018.04.010>
- BenMoussa-Dahmen, I., Chtourou, H., Rezgui, F., Sayadi, S., & Dhouib, A. (2016).

- Salinity stress increases lipid, secondary metabolites and enzyme activity in *Amphora subtropica* and *Dunaliella* sp. for biodiesel production. *Bioresource Technology*, 218, 816–825. <https://doi.org/10.1016/j.biortech.2016.07.022>
- Biller, P., & Ross, A. B. (2011). Potential yields and properties of oil from the hydrothermal liquefaction of microalgae with different biochemical content. *Bioresource Technology*, 102(1), 215–225. <https://doi.org/10.1016/j.biortech.2010.06.028>
- Biller, P., & Ross, A. B. (2016). Production of biofuels via hydrothermal conversion. In *Handbook of Biofuels Production: Processes and Technologies: Second Edition*. Elsevier Ltd. <https://doi.org/10.1016/B978-0-08-100455-5.00017-5>
- Biller, P., Ross, A. B., Skill, S. C., Lea-Langton, A., Balasundaram, B., Hall, C., Riley, R., & Llewellyn, C. A. (2012). Nutrient recycling of aqueous phase for microalgae cultivation from the hydrothermal liquefaction process. *Algal Research*, 1(1), 70–76. <https://doi.org/10.1016/j.algal.2012.02.002>
- Bonvicini, C., Faraone, S. V., & Scassellati, C. (2016). Attention-deficit hyperactivity disorder in adults: A systematic review and meta-analysis of genetic, pharmacogenetic and biochemical studies. *Molecular Psychiatry*, 21(7), 872–884. <https://doi.org/10.1038/mp.2016.74>
- Bowler, C., & Falciatore, A. (2014). The molecular life of diatoms. *Marine Genomics*, 16(1), 1–3. <https://doi.org/10.1016/j.margen.2014.07.002>
- Byreddy, A. R., Gupta, A., Barrow, C. J., & Puri, M. (2016). A quick colorimetric method for total lipid quantification in microalgae. *Journal of Microbiological Methods*, 125, 28–32. <https://doi.org/10.1016/j.mimet.2016.04.002>
- Campos, H., Boeing, W. J., Dungan, B. N., & Schaub, T. (2014). Cultivating the marine microalga *Nannochloropsis salina* under various nitrogen sources: Effect on

- biovolume yields, lipid content and composition, and invasive organisms. *Biomass and Bioenergy*, 66, 301–307. <https://doi.org/10.1016/j.biombioe.2014.04.005>
- Che, H., Zhou, M., Zhang, T., Zhang, L., Ding, L., Yanagita, T., Xu, J., Xue, C., & Wang, Y. (2018). EPA enriched ethanolamine plasmalogens significantly improve cognition of Alzheimer's disease mouse model by suppressing  $\beta$ -amyloid generation. *Journal of Functional Foods*, 41, 9–18. <https://doi.org/10.1016/j.jff.2017.12.016>
- Chen, J.-R., Hsu, S.-F., Hsu, C.-D., Hwang, L.-H., & Yang, S.-C. (2004). Dietary patterns and blood fatty acid composition in children with attention-deficit hyperactivity disorder in Taiwan. *The Journal of Nutritional Biochemistry*, 15(8), 467–472. <https://doi.org/10.1016/j.jnutbio.2004.01.008>
- Chen, Y. C. (2012). The biomass and total lipid content and composition of twelve species of marine diatoms cultured under various environments. *Food Chemistry*, 131(1), 211–219. <https://doi.org/10.1016/j.foodchem.2011.08.062>
- Cheng, J. J., & Timilsina, G. R. (2011). Status and barriers of advanced biofuel technologies: A review. *Renewable Energy*, 36(12), 3541–3549. <https://doi.org/10.1016/j.renene.2011.04.031>
- Chtourou, H., Dahmen, I., Jebali, A., Karray, F., Hassairi, I., Abdelkafi, S., Ayadi, H., Sayadi, S., & Dhoub, A. (2015). Characterization of *Amphora* sp., a newly isolated diatom wild strain, potentially usable for biodiesel production. *Bioprocess and Biosystems Engineering*, 38(7), 1381–1392. <https://doi.org/10.1007/s00449-015-1379-6>
- Cointet, E., Wielgosz-Collin, G., Méléder, V., & Gonçalves, O. (2019). Lipids in benthic diatoms: A new suitable screening procedure. *Algal Research*, 39(February), 101425. <https://doi.org/10.1016/j.algal.2019.101425>

- Conde, E., Balboa, E. M., Parada, M., & Falqué, E. (2013). Algal proteins, peptides and amino acids. In *Functional Ingredients from Algae for Foods and Nutraceuticals* (pp. 135–180). <https://doi.org/10.1533/9780857098689.1.135>
- Das, P., Thaher, M. I., Khan, S., AbdulQuadir, M., Chaudhary, A. K., Alghasal, G., & Al-Jabri, H. (2019). Comparison of biocrude oil production from self-settling and non-settling microalgae biomass produced in the Qatari desert environment. *International Journal of Environmental Science and Technology*, *16*(11), 7443–7454. <https://doi.org/10.1007/s13762-019-02364-w>
- Das, Probir, Khan, S., AbdulQuadir, M., Thaher, M., Waqas, M., Easa, A., Attia, E. S. M., & Al-Jabri, H. (2020). Energy recovery and nutrients recycling from municipal sewage sludge. *Science of the Total Environment*, *715*, 136775. <https://doi.org/10.1016/j.scitotenv.2020.136775>
- Das, Probir, Khan, S., Thaher, M., AbdulQuadir, M., Hoekman, S. K., & Al-Jabri, H. (2019). Effect of harvesting methods on the energy requirement of *Tetraselmis* sp. biomass production and biocrude yield and quality. *Bioresource Technology*, *284*(February), 9–15. <https://doi.org/10.1016/j.biortech.2019.03.118>
- Das, Probir, Thaher, M. I., Hakim, M. A. Q. M. A., Al-Jabri, H. M. S. J., & Alghasal, G. S. H. S. (2016). A comparative study of the growth of *Tetraselmis* sp. in large scale fixed depth and decreasing depth raceway ponds. *Bioresource Technology*, *216*, 114–120. <https://doi.org/10.1016/j.biortech.2016.05.058>
- Dasilva, G., Pazos, M., García-Egido, E., Gallardo, J. M., Rodríguez, I., Cela, R., & Medina, I. (2015). Healthy effect of different proportions of marine  $\omega$ -3 PUFAs EPA and DHA supplementation in Wistar rats: Lipidomic biomarkers of oxidative stress and inflammation. *The Journal of Nutritional Biochemistry*, *26*(11), 1385–1392. <https://doi.org/https://doi.org/10.1016/j.jnutbio.2015.07.007>

- Dawczynski, C., Dittrich, M., Neumann, T., Goetze, K., Welzel, A., Oelzner, P., Völker, S., Schaible, A. M., Troisi, F., Thomas, L., Pace, S., Koeberle, A., Werz, O., Schlattmann, P., Lorkowski, S., & Jahreis, G. (2018). Docosahexaenoic acid in the treatment of rheumatoid arthritis: A double-blind, placebo-controlled, randomized cross-over study with microalgae vs. sunflower oil. *Clinical Nutrition*, 37(2), 494–504. <https://doi.org/10.1016/j.clnu.2017.02.021>
- Dias, N., Mota, D., Nicolau, A., & Mota, M. (2018). Monitoring *Amphora* sp. growth by flow cytometry. In *Diatom Research* (Vol. 33, Issue 3, pp. 405–411). <https://doi.org/10.1080/0269249X.2018.1523231>
- Dubois, M., Gilles, K., Hamilton, J. K., Rebers, P. A., & Smith, F. (1951). A colorimetric method for the determination of sugars. *Nature*, 168(4265), 167. <https://doi.org/10.1038/168167a0>
- Duong, V. T., Thomas-Hall, S. R., & Schenk, P. M. (2015). Growth and lipid accumulation of microalgae from fluctuating brackish and sea water locations in South East Queensland—Australia. *Frontiers in Plant Science*. <https://doi.org/10.3389/fpls.2015.00359>
- Eboibi, B. E., Lewis, D. M., Ashman, P. J., & Chinnasamy, S. (2014). Effect of operating conditions on yield and quality of biocrude during hydrothermal liquefaction of halophytic microalga *Tetraselmis* sp. *Bioresource Technology*, 170, 20–29. <https://doi.org/10.1016/j.biortech.2014.07.083>
- Galadima, A., & Muraza, O. (2018). Hydrothermal liquefaction of algae and bio-oil upgrading into liquid fuels: Role of heterogeneous catalysts. *Renewable and Sustainable Energy Reviews*, 81(January 2017), 1037–1048. <https://doi.org/10.1016/j.rser.2017.07.034>

- Garcia Alba, L., Torri, C., Samorì, C., Van Der Spek, J., Fabbri, D., Kersten, S. R. A., & Brilman, D. W. F. (2012). Hydrothermal treatment (HTT) of microalgae: Evaluation of the process as conversion method in an algae biorefinery concept. *Energy and Fuels*, *26*(1), 642–657. <https://doi.org/10.1021/ef201415s>
- Gollakota, A. R. K., Kishore, N., & Gu, S. (2018). A review on hydrothermal liquefaction of biomass. *Renewable and Sustainable Energy Reviews*, *81*(June 2017), 1378–1392. <https://doi.org/10.1016/j.rser.2017.05.178>
- Granado-Casas, M., & Mauricio, D. (2019). *Chapter 14 - Oleic Acid in the Diet and What It Does: Implications for Diabetes and Its Complications* (R. R. Watson & V. R. B. T.-B. F. as D. I. for D. (Second E. Preedy (eds.); pp. 211–229). Academic Press. <https://doi.org/https://doi.org/10.1016/B978-0-12-813822-9.00014-X>
- Gu, X., Martinez-Fernandez, J. S., Pang, N., Fu, X., & Chen, S. (2020). Recent development of hydrothermal liquefaction for algal biorefinery. *Renewable and Sustainable Energy Reviews*, *121*(December 2019). <https://doi.org/10.1016/j.rser.2020.109707>
- Guo, B., Walter, V., Hornung, U., & Dahmen, N. (2019). Hydrothermal liquefaction of *Chlorella vulgaris* and *Nannochloropsis gaditana* in a continuous stirred tank reactor and hydrotreating of biocrude by nickel catalysts. *Fuel Processing Technology*, *191*(April), 168–180. <https://doi.org/10.1016/j.fuproc.2019.04.003>
- Guo, B., Yang, B., Silve, A., Akaberi, S., Scherer, D., Papachristou, I., Frey, W., Hornung, U., & Dahmen, N. (2019). Hydrothermal liquefaction of residual microalgae biomass after pulsed electric field-assisted valuables extraction. *Algal Research*, *43*(April), 101650. <https://doi.org/10.1016/j.algal.2019.101650>
- Guo, X., Li, K., Li, J., & Li, D. (2019). Effects of EPA and DHA on blood pressure and inflammatory factors: a meta-analysis of randomized controlled trials. *Critical*



- Reviews in Food Science and Nutrition*, 59(20), 3380–3393.  
<https://doi.org/10.1080/10408398.2018.1492901>
- Hable, R. D., Alimoradi, S., Sturm, B. S. M., & Stagg-Williams, S. M. (2019). Simultaneous solid and biocrude product transformations from the hydrothermal treatment of high pH-induced flocculated algae at varying Ca concentrations. *Algal Research*. <https://doi.org/10.1016/j.algal.2019.101501>
- Han, Y., Hoekman, S. K., Cui, Z., Jena, U., & Das, P. (2019). Hydrothermal liquefaction of marine microalgae biomass using co-solvents. *Algal Research*, 38(January), 101421. <https://doi.org/10.1016/j.algal.2019.101421>
- He, S., Zhao, M., Wang, J., Cheng, Z., Yan, B., & Chen, G. (2020). Hydrothermal liquefaction of low-lipid algae *Nannochloropsis* sp. and *Sargassum* sp.: Effect of feedstock composition and temperature. *Science of the Total Environment*, 712, 135677. <https://doi.org/10.1016/j.scitotenv.2019.135677>
- Heras-Sandoval, D., Pedraza-Chaverri, J., & Pérez-Rojas, J. M. (2016). Role of docosahexaenoic acid in the modulation of glial cells in Alzheimer's disease. *Journal of Neuroinflammation*, 13(1), 61. <https://doi.org/10.1186/s12974-016-0525-7>
- Hu, Yan, Hall, C. A. S., Wang, J., Feng, L., & Poisson, A. (2013). Energy Return on Investment (EROI) of China's conventional fossil fuels: Historical and future trends. *Energy*. <https://doi.org/10.1016/j.energy.2013.01.067>
- Hu, Yulin, Gong, M., Feng, S., Xu, C. (Charles), & Bassi, A. (2019). A review of recent developments of pre-treatment technologies and hydrothermal liquefaction of microalgae for bio-crude oil production. *Renewable and Sustainable Energy Reviews*, 101(April 2018), 476–492. <https://doi.org/10.1016/j.rser.2018.11.037>
- Hubbard, A. (2007). Surfactants in Personal Care Products and Decorative Cosmetics,

- third ed., Linda D. Rhein, Mitchell Schlossman, Anthony O'Lenick, P. Somasundaran (Eds.), CRC Press, Boca Raton, FL (2007), 480 pp. *Journal of Colloid and Interface Science*, 307(2), 582.  
<https://doi.org/https://doi.org/10.1016/j.jcis.2006.12.065>
- Jiang, Y., Laverty, K. S., Brown, J., Nunez, M., Brown, L., Chagoya, J., Burow, M., & Quigg, A. (2014). Effects of fluctuating temperature and silicate supply on the growth, biochemical composition and lipid accumulation of *Nitzschia* sp. *Bioresource Technology*, 154, 336–344.  
<https://doi.org/10.1016/j.biortech.2013.12.068>
- Kazemi Shariat Panahi, H., Tabatabaei, M., Aghbashlo, M., Dehghani, M., Rehan, M., & Nizami, A. S. (2019). Recent updates on the production and upgrading of bio-crude oil from microalgae. *Bioresource Technology Reports*, 7(April), 100216.  
<https://doi.org/10.1016/j.biteb.2019.100216>
- Klin, M., Pniewski, F., & Latała, A. (2020). Growth phase-dependent biochemical composition of green microalgae: Theoretical considerations for biogas production. *Bioresource Technology*, 303(November 2019).  
<https://doi.org/10.1016/j.biortech.2020.122875>
- Kunene, P. N., & Mahlambi, P. N. (2020). Optimization and application of ultrasonic extraction and Soxhlet extraction followed by solid phase extraction for the determination of triazine pesticides in soil and sediment. *Journal of Environmental Chemical Engineering*, 8(2), 103665. <https://doi.org/10.1016/j.jece.2020.103665>
- Leong, W. H., Lim, J. W., Lam, M. K., Uemura, Y., & Ho, Y. C. (2018). Third generation biofuels: A nutritional perspective in enhancing microbial lipid production. *Renewable and Sustainable Energy Reviews*, 91(April), 950–961.  
<https://doi.org/10.1016/j.rser.2018.04.066>

- Levitan, O., Dinamarca, J., Hochman, G., & Falkowski, P. G. (2014). Diatoms: A fossil fuel of the future. *Trends in Biotechnology*, 32(3), 117–124. <https://doi.org/10.1016/j.tibtech.2014.01.004>
- Li, Z., & Savage, P. E. (2013). Feedstocks for fuels and chemicals from algae: Treatment of crude bio-oil over HZSM-5. In *Algal Research* (Vol. 2, Issue 2, pp. 154–163). <https://doi.org/10.1016/j.algal.2013.01.003>
- LICHTENTHALER, H. K., & WELLBURN, A. R. (1983). Determinations of total carotenoids and chlorophylls a and b of leaf extracts in different solvents. *Biochemical Society Transactions*, 11(5), 591–592. <https://doi.org/10.1042/bst0110591>
- Lin, Q., & Lin, J. (2011). Effects of nitrogen source and concentration on biomass and oil production of a *Scenedesmus rubescens* like microalga. *Bioresource Technology*, 102(2), 1615–1621. <https://doi.org/10.1016/j.biortech.2010.09.008>
- Liu, R., Tian, W., Kong, S., Meng, Y., Wang, H., & Zhang, J. (2018). Effects of inorganic and organic acid pretreatments on the hydrothermal liquefaction of municipal secondary sludge. *Energy Conversion and Management*. <https://doi.org/10.1016/j.enconman.2018.08.058>
- López Barreiro, D., Martin-Martinez, F. J., Torri, C., Prins, W., & Buehler, M. J. (2018). Molecular characterization and atomistic model of biocrude oils from hydrothermal liquefaction of microalgae. *Algal Research*, 35(August), 262–273. <https://doi.org/10.1016/j.algal.2018.08.034>
- López Barreiro, D., Prins, W., Ronsse, F., & Brilman, W. (2013). Hydrothermal liquefaction (HTL) of microalgae for biofuel production: State of the art review and future prospects. *Biomass and Bioenergy*, 53(0), 113–127. <https://doi.org/10.1016/j.biombioe.2012.12.029>

- López, C. V. G., del Carmen Cerón García, M., Fernández, F. G. A., Bustos, C. S., Chisti, Y., & Sevilla, J. M. F. (2010). Protein measurements of microalgal and cyanobacterial biomass. *Bioresource Technology*, *101*(19), 7587–7591. <https://doi.org/10.1016/j.biortech.2010.04.077>
- Maity, J. P., Bundschuh, J., Chen, C. Y., & Bhattacharya, P. (2014). Microalgae for third generation biofuel production, mitigation of greenhouse gas emissions and wastewater treatment: Present and future perspectives - A mini review. *Energy*, *78*, 104–113. <https://doi.org/10.1016/j.energy.2014.04.003>
- Mandal, S., & Mallick, N. (2014). Microalgae: The Tiny Microbes with a Big Impact. In *Bioenergy Research: Advances and Applications*. Elsevier. <https://doi.org/10.1016/B978-0-444-59561-4.00011-5>
- Mathimani, T., Baldinelli, A., Rajendran, K., Prabakar, D., Matheswaran, M., Pieter van Leeuwen, R., & Pugazhendhi, A. (2019). Review on cultivation and thermochemical conversion of microalgae to fuels and chemicals: Process evaluation and knowledge gaps. *Journal of Cleaner Production*, *208*, 1053–1064. <https://doi.org/10.1016/j.jclepro.2018.10.096>
- Mathimani, T., & Pugazhendhi, A. (2019). Utilization of algae for biofuel, bio-products and bio-remediation. *Biocatalysis and Agricultural Biotechnology*, *17*(November 2018), 326–330. <https://doi.org/10.1016/j.bcab.2018.12.007>
- Menegazzo, M. L., & Fonseca, G. G. (2019). Biomass recovery and lipid extraction processes for microalgae biofuels production: A review. *Renewable and Sustainable Energy Reviews*, *107*(February), 87–107. <https://doi.org/10.1016/j.rser.2019.01.064>
- Meng, X., Yang, J., Xu, X., Zhang, L., Nie, Q., & Xian, M. (2009). Biodiesel production from oleaginous microorganisms. *Renewable Energy*, *34*(1), 1–5.

<https://doi.org/10.1016/j.renene.2008.04.014>

Mishra, S., & Mohanty, K. (2020). Co-HTL of domestic sewage sludge and wastewater treatment derived microalgal biomass – An integrated biorefinery approach for sustainable biocrude production. *Energy Conversion and Management*.  
<https://doi.org/10.1016/j.enconman.2019.112312>

Mohan, S. V., Devi, M. P., Subhash, G. V., & Chandra, R. (2013). Algae Oils as Fuels. In *Biofuels from Algae*. <https://doi.org/10.1016/B978-0-444-59558-4.00008-5>

Nayak, M., Suh, W. I., Chang, Y. K., & Lee, B. (2019). Exploration of two-stage cultivation strategies using nitrogen starvation to maximize the lipid productivity in *Chlorella* sp. HS2. *Bioresource Technology*, 276(October 2018), 110–118.  
<https://doi.org/10.1016/j.biortech.2018.12.111>

Niccolai, A., Chini Zittelli, G., Rodolfi, L., Biondi, N., & Tredici, M. R. (2019). Microalgae of interest as food source: Biochemical composition and digestibility. *Algal Research*, 42(April). <https://doi.org/10.1016/j.algal.2019.101617>

Obeid, F., Van, T. C., Horchler, E. J., Guo, Y., Verma, P., Miljevic, B., Brown, R. J., Ristovski, Z., Bodisco, T. A., & Rainey, T. (2020). Engine performance and emissions of high nitrogen-containing fuels. *Fuel*, 264(November 2019), 116805.  
<https://doi.org/10.1016/j.fuel.2019.116805>

Ördög, V., Stirk, W. A., Bálint, P., Aremu, A. O., Okem, A., Lovász, C., Molnár, Z., & van Staden, J. (2016). Effect of temperature and nitrogen concentration on lipid productivity and fatty acid composition in three *Chlorella* strains. *Algal Research*, 16, 141–149. <https://doi.org/10.1016/j.algal.2016.03.001>

Ortea, I., González-Fernández, M. J., Ramos-Bueno, R. P., & Guil-Guerrero, J. L. (2018). Proteomics Study Reveals That Docosaehaenoic and Arachidonic Acids Exert Different In Vitro Anticancer Activities in Colorectal Cancer Cells. *Journal*

- of Agricultural and Food Chemistry*, 66(24), 6003–6012.  
<https://doi.org/10.1021/acs.jafc.8b00915>
- Palomino, A., Godoy-Silva, R. D., Raikova, S., & Chuck, C. J. (2020). The storage stability of biocrude obtained by the hydrothermal liquefaction of microalgae. *Renewable Energy*, 145, 1720–1729.  
<https://doi.org/10.1016/j.renene.2019.07.084>
- Parsa, M., Jalilzadeh, H., Pazoki, M., Ghasemzadeh, R., & Abduli, M. A. (2018). Hydrothermal liquefaction of *Gracilaria gracilis* and *Cladophora glomerata* macroalgae for biocrude production. *Bioresource Technology*.  
<https://doi.org/10.1016/j.biortech.2017.10.059>
- Parveez, G. K. A., Rasid, O. A., Hashim, A. T., Ishak, Z., Rosli, S. K., & Sambanthamurthi, R. (2012). 4 - *Tissue Culture and Genetic Engineering of Oil Palm* (O.-M. Lai, C.-P. Tan, & C. C. B. T.-P. O. Akoh (eds.); pp. 87–135). AOCS Press. <https://doi.org/https://doi.org/10.1016/B978-0-9818936-9-3.50007-1>
- Patrick, R. P., & Ames, B. N. (2015). Vitamin D and the omega-3 fatty acids control serotonin synthesis and action, part 2: relevance for ADHD, bipolar disorder, schizophrenia, and impulsive behavior. *The FASEB Journal*, 29(6), 2207–2222.  
<https://doi.org/10.1096/fj.14-268342>
- Rajaram, M. G., Nagaraj, S., Manjunath, M., Boopathy, A. B., Kurinjimalar, C., Rengasamy, R., Jayakumar, T., Sheu, J. R., & Li, J. Y. (2018). Biofuel and biochemical analysis of amphora coffeaeformis RR03, a novel marine diatom, cultivated in an open raceway pond. *Energies*, 11(6), 1–13.  
<https://doi.org/10.3390/en11061341>
- Ren, R., Han, X., Zhang, H., Lin, H., Zhao, J., Zheng, Y., & Wang, H. (2018). High yield bio-oil production by hydrothermal liquefaction of a hydrocarbon-rich

- microalgae and biocrude upgrading. *Carbon Resources Conversion*, 1(2), 153–159. <https://doi.org/10.1016/j.crcon.2018.07.008>
- Robert A. Andersen. (2005). Algal culturing techniques. In *Elsevier* (Vol. 43, Issue 02). Elsevier. <https://doi.org/10.5860/choice.43-0925>
- Sahin, M. S., Khazi, M. I., Demirel, Z., & Dalay, M. C. (2019). Variation in growth, fucoxanthin, fatty acids profile and lipid content of marine diatoms *Nitzschia* sp. and *Nanofrustulum shiloi* in response to nitrogen and iron. *Biocatalysis and Agricultural Biotechnology*, 17(October 2018), 390–398. <https://doi.org/10.1016/j.bcab.2018.12.023>
- Sajjadi, B., Chen, W. Y., Raman, A. A. A., & Ibrahim, S. (2018). Microalgae lipid and biomass for biofuel production: A comprehensive review on lipid enhancement strategies and their effects on fatty acid composition. *Renewable and Sustainable Energy Reviews*, 97(June), 200–232. <https://doi.org/10.1016/j.rser.2018.07.050>
- Sekikawa, A., Mahajan, H., Kadowaki, S., Hisamatsu, T., Miyagawa, N., Fujiyoshi, A., Kadota, A., Maegawa, H., Murata, K., Miura, K., Edmundowicz, D., Ueshima, H., & Group, for the S. R. (2019). Association of blood levels of marine omega-3 fatty acids with coronary calcification and calcium density in Japanese men. *European Journal of Clinical Nutrition*, 73(5), 783–792. <https://doi.org/10.1038/s41430-018-0242-7>
- Shuba, E. S., & Kifle, D. (2018). Microalgae to biofuels: ‘Promising’ alternative and renewable energy, review. *Renewable and Sustainable Energy Reviews*, 81(April 2016), 743–755. <https://doi.org/10.1016/j.rser.2017.08.042>
- Sun, P., Wong, C. C., Li, Y., He, Y., Mao, X., Wu, T., Ren, Y., & Chen, F. (2019). A novel strategy for isolation and purification of fucoxanthinol and fucoxanthin from the diatom *Nitzschia laevis*. *Food Chemistry*, 277(April 2018), 566–572.

<https://doi.org/10.1016/j.foodchem.2018.10.133>

- Tian, C., Li, B., Liu, Z., Zhang, Y., & Lu, H. (2014). Hydrothermal liquefaction for algal biorefinery: A critical review. *Renewable and Sustainable Energy Reviews*, 38, 933–950. <https://doi.org/10.1016/j.rser.2014.07.030>
- Tsuchiya, Y., Yanagimoto, K., Nakazato, K., Hayamizu, K., & Ochi, E. (2016). Eicosapentaenoic and docosahexaenoic acids-rich fish oil supplementation attenuates strength loss and limited joint range of motion after eccentric contractions: a randomized, double-blind, placebo-controlled, parallel-group trial. *European Journal of Applied Physiology*, 116(6), 1179–1188. <https://doi.org/10.1007/s00421-016-3373-3>
- Tzanetis, K. F., Posada, J. A., & Ramirez, A. (2017). Analysis of biomass hydrothermal liquefaction and biocrude-oil upgrading for renewable jet fuel production: The impact of reaction conditions on production costs and GHG emissions performance. *Renewable Energy*, 113, 1388–1398. <https://doi.org/10.1016/j.renene.2017.06.104>
- Uriarte, I., Roberts, R., & Farías, A. (2006). The effect of nitrate supplementation on the biochemical composition of benthic diatoms and the growth and survival of post-larval abalone. *Aquaculture*, 261(1), 423–429. <https://doi.org/10.1016/j.aquaculture.2006.08.007>
- Vardon, D. R., Sharma, B. K., Scott, J., Yu, G., Wang, Z., Schideman, L., Zhang, Y., & Strathmann, T. J. (2011). Chemical properties of biocrude oil from the hydrothermal liquefaction of Spirulina algae, swine manure, and digested anaerobic sludge. *Bioresource Technology*, 102(17), 8295–8303. <https://doi.org/10.1016/j.biortech.2011.06.041>
- Vella, F. M., Sardo, A., Gallo, C., Landi, S., Fontana, A., & d’Ippolito, G. (2019).



- Annual outdoor cultivation of the diatom *Thalassiosira weissflogii*: productivity, limits and perspectives. *Algal Research*, 42(June 2018), 101553. <https://doi.org/10.1016/j.algal.2019.101553>
- Wall, R., Ross, R. P., Fitzgerald, G. F., & Stanton, C. (2010). Fatty acids from fish: the anti-inflammatory potential of long-chain omega-3 fatty acids. *Nutrition Reviews*, 68(5), 280–289. <https://doi.org/10.1111/j.1753-4887.2010.00287.x>
- Wang, J. K., & Seibert, M. (2017). Prospects for commercial production of diatoms. *Biotechnology for Biofuels*, 10(1), 1–14. <https://doi.org/10.1186/s13068-017-0699-y>
- Yassine, H. N., Braskie, M. N., Mack, W. J., Castor, K. J., Fonteh, A. N., Schneider, L. S., Harrington, M. G., & Chui, H. C. (2017). Association of Docosahexaenoic Acid Supplementation With Alzheimer Disease Stage in Apolipoprotein E  $\epsilon$ 4 Carriers: A Review. *JAMA Neurology*, 74(3), 339–347. <https://doi.org/10.1001/jamaneurol.2016.4899>
- Yodsuan, N., Sawayama, S., & Sirisansaneeyakul, S. (2017). Effect of nitrogen concentration on growth, lipid production and fatty acid profiles of the marine diatom *Phaeodactylum tricornutum*. *Agriculture and Natural Resources*, 51(3), 190–197. <https://doi.org/10.1016/j.anres.2017.02.004>
- Yoo, G., Park, M. S., Yang, J. W., & Choi, M. (2015). Lipid content in microalgae determines the quality of biocrude and Energy Return On Investment of hydrothermal liquefaction. *Applied Energy*. <https://doi.org/10.1016/j.apenergy.2015.07.020>
- Yum, H.-W., Na, H.-K., & Surh, Y.-J. (2016). Anti-inflammatory effects of docosahexaenoic acid: Implications for its cancer chemopreventive potential. *Seminars in Cancer Biology*, 40–41, 141–159.

<https://doi.org/https://doi.org/10.1016/j.semcancer.2016.08.004>

Zhang, Y., & Chen, W.-T. (2018). 5 - *Hydrothermal liquefaction of protein-containing feedstocks* (L. B. T.-D. T. L. for E. A. Rosendahl (ed.); pp. 127–168). Woodhead

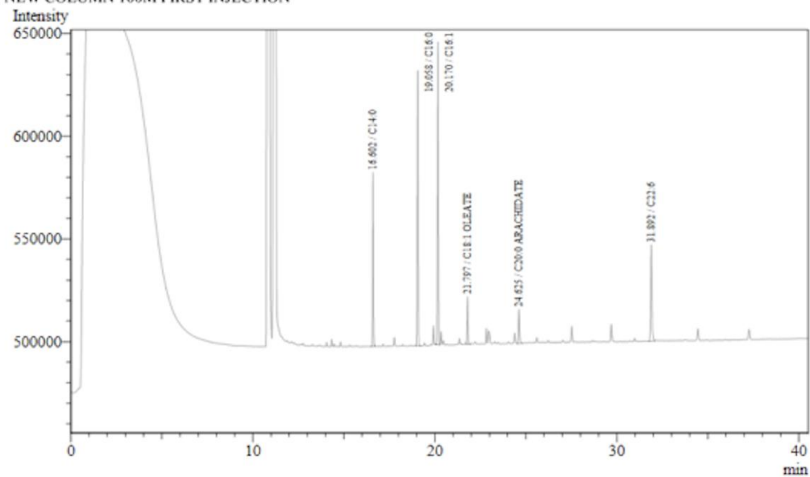
Publishing. <https://doi.org/https://doi.org/10.1016/B978-0-08-101029-7.00004-7>

Zulu, N. N., Zienkiewicz, K., Vollheyde, K., & Feussner, I. (2018). Current trends to comprehend lipid metabolism in diatoms. *Progress in Lipid Research*,

70(December 2017), 1–16. <https://doi.org/10.1016/j.plipres.2018.03.001>

## APPENDIX: GC/MS CHROMATOGRAM OF (FAMES)

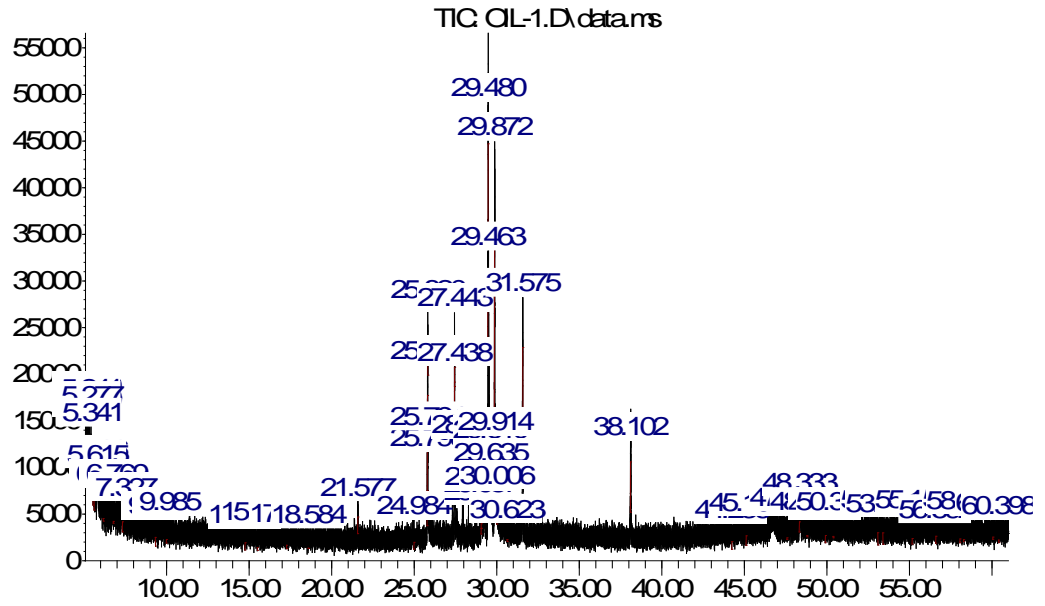
Data Name : C:\GCsolution\Data\Sara\Sara sample integrated.gcd  
 Method Name : C:\GCsolution\Data\Project1\GC\method\FAME\_STD\_08SEP2019.gcm  
 [Description]  
 NEW COLUMN 100M FIRST INJECTION



Peak#	Ret.Time	Area	Height	Conc.	Unit	Mark	ID#	Cmpd Name
1	16.602	278233	83866	198.904	PPM		1	C14:0
2	19.058	462905	132603	272.816	PPM		3	C16:0
3	20.170	515858	145559	399.971	PPM		4	C16:1
4	21.797	85899	23054	-1.804	PPM	V	6	C18:1 OLEATE
5	24.625	67612	16317	47.173	PPM		10	C20:0 ARACHIDATE
6	31.892	221022	46638	135.321	PPM		19	C22:6
<b>Total</b>		<b>1631529</b>	<b>448037</b>					

## APPENDIX: GC/MS CHROMATOGRAM OF HYDROCARBONS IN THE BIOCRUDE

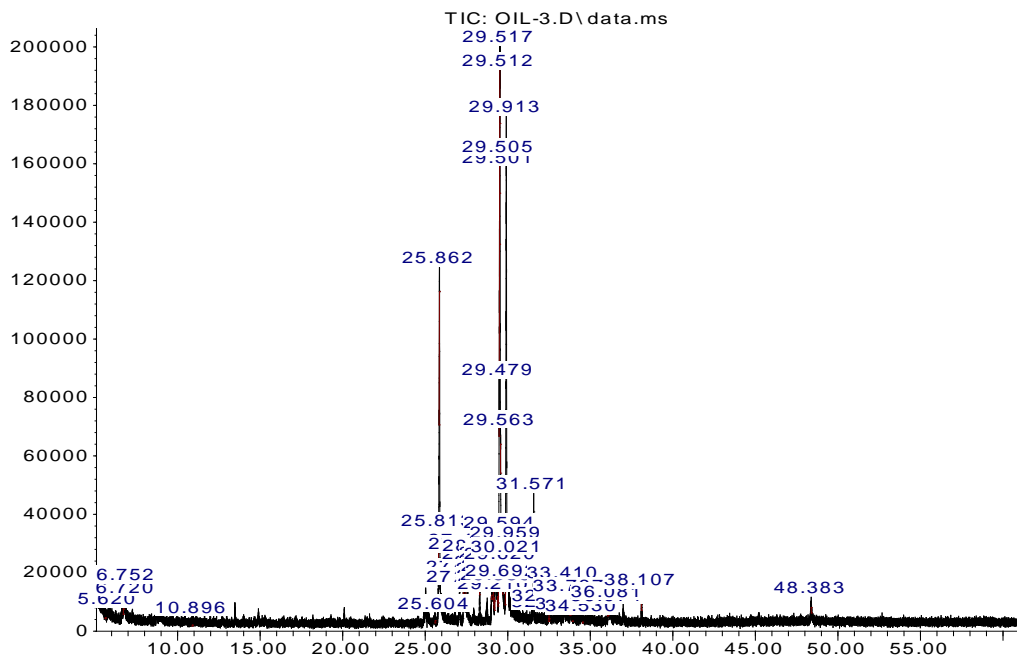
Abundance



Time-->

Biocrude processed at 300 °C HTL

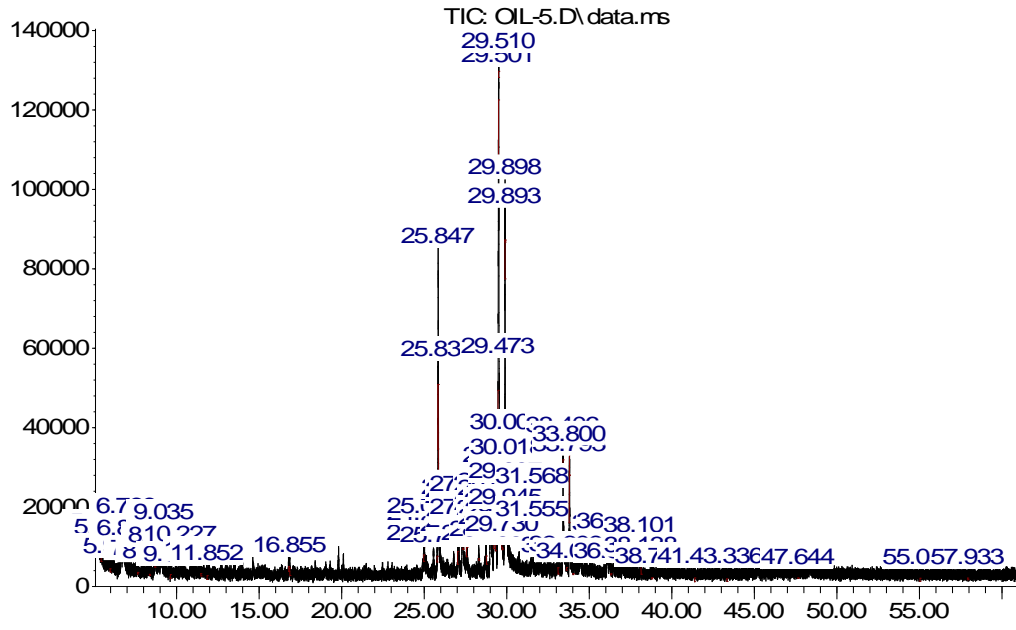
Abundance



Time-->

Biocrude processed at 325 °C HTL

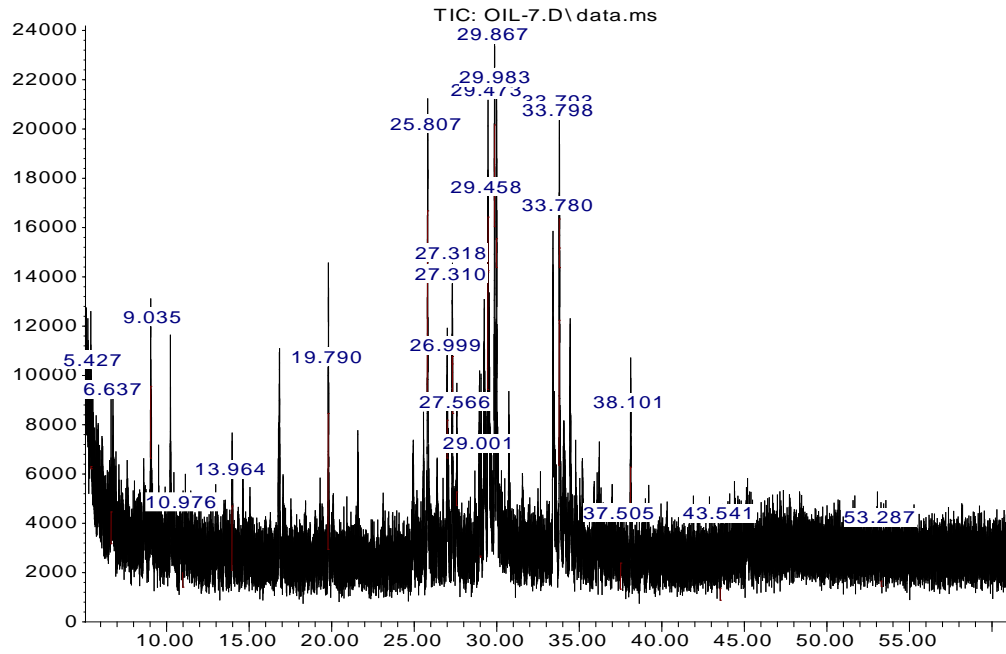
Abundance



Time-->

Biocrude processed at 350 °C HTL

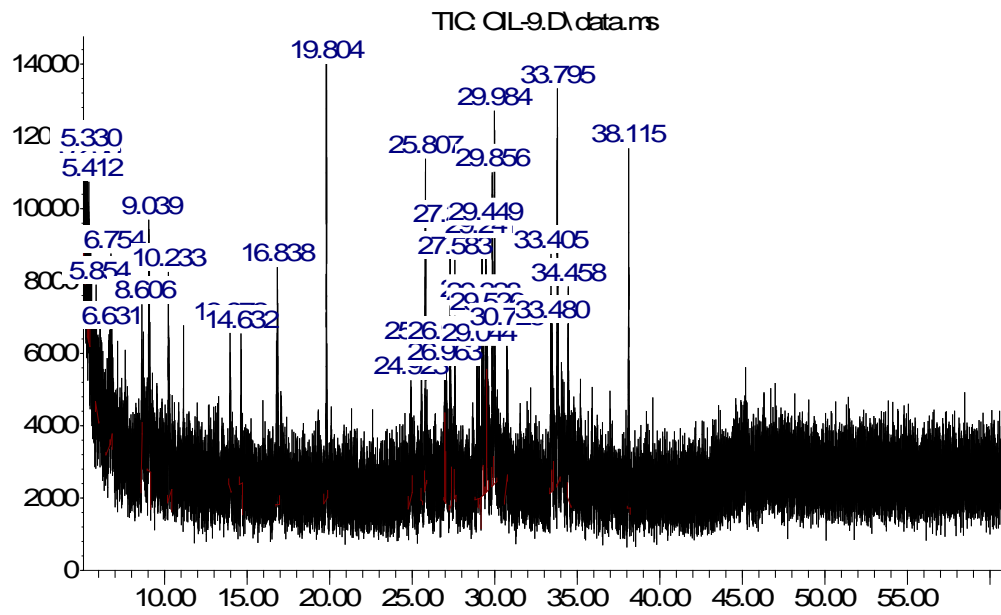
Abundance



Time-->

Biocrude processed at 375 °C HTL

Abundance



Time-->

Biocrude processed at 375 °C HTL

### APPENDIX: FUCOXANTHIN WAVELENGTH

